



# Central role of glycosylation processes in human genetic susceptibility to SARS-CoV-2 infections with Omicron variants

Received: 20 November 2024

A list of authors and their affiliations appears at the end of the paper

Accepted: 12 December 2025

Published online: 22 January 2026

Check for updates

The host genetics of severe acute respiratory syndrome coronavirus 2 (SARS-CoV-2) have previously been studied based on cases from the earlier waves of the pandemic in 2020 and 2021, identifying 51 genomic loci associated with infection and/or severity. SARS-CoV-2 has shown rapid sequence evolution, increasing transmissibility, particularly for Omicron variants, which raises the question of whether this affected the host genetic factors. We performed a genome-wide association study of SARS-CoV-2 infection with Omicron variants, including more than 150,000 cases from four cohorts. We identified 13 genome-wide significant loci, of which only five were previously described as associated with SARS-CoV-2 infection. The strongest signal was a single nucleotide polymorphism in an intron of *ST6GAL1*, a gene affecting immune development and function, connected to three other associated loci (harboring *MUC1*, *MUC5AC* and *MUC16*) through O-glycan biosynthesis. Our study provides robust evidence for individual genetic variation related to glycosylation, translating into susceptibility to SARS-CoV-2 infections with Omicron variants.

According to data from the World Health Organization, SARS-CoV-2 has by now caused more than 770 million cases of COVID-19, resulting in more than seven million deaths<sup>1</sup>. The largest genetic study on susceptibility to SARS-CoV-2 infection was a genome-wide association study (GWAS) by the COVID-19 Host Genetics Initiative (HGI), meta-analyzing up to 219,692 cases and over three million controls, which identified 51 genetic loci<sup>2</sup> associated with infection and/or two other outcomes related to COVID-19 disease severity. However, that study was built on a data freeze from December 2021, just after the detection of Omicron in November 2021, and therefore only included infections with earlier (pre-Omicron) SARS-CoV-2 variants. The evolution of the virus gave rise to multiple mutations that affected, among others, the transmissibility of the virus<sup>3</sup>. Omicron variants showed more mutations than earlier variants and, within a few months, infected far more individuals worldwide than all the earlier variants combined.

Given these substantial changes observed in the virus, we decided to investigate the corresponding host genetics by performing a GWAS of SARS-CoV-2 infection with Omicron variants in >150,000 cases and >500,000 controls without known SARS-CoV-2 infection by combining data from four cohorts in a meta-analysis.

## Results

### GWAS of Omicron infection versus no infection

In our main analysis, we compared SARS-CoV-2 infection with Omicron variants (proxied by the first reported infection observed in a period during which Omicron variants were dominating in the study cohorts, which was after the start of 2022) versus controls with no known SARS-CoV-2 infection, using data from electronic health records, viral testing or questionnaire data in the covered time period (see Methods for further details). To simplify matters, genetic variants are denoted as single nucleotide polymorphisms (SNPs) throughout the paper, so that the term 'variant' always refers to variation in SARS-CoV-2.

We performed a meta-analysis of four GWAS with a total of 151,825 cases and 556,568 controls (see Fig. 1 for Manhattan plot) and identified 13 genome-wide significant loci, of which eight represent novel associations for SARS-CoV-2 infection (Table 1). Four of the corresponding lead SNPs had proxies among the previously reported SNPs associated with SARS-CoV-2 infection related to earlier variants ( $r^2 > 0.6$ ), and for the *SLC6A20* locus, the lead SNP reported for the earlier variants was in the 95% credible set of our GWAS signal ([rs73062389](https://doi.org/10.1101/2389),  $P = 8.9 \times 10^{-33}$  in our study; see Supplementary Fig. 1). Two of these loci had been assigned

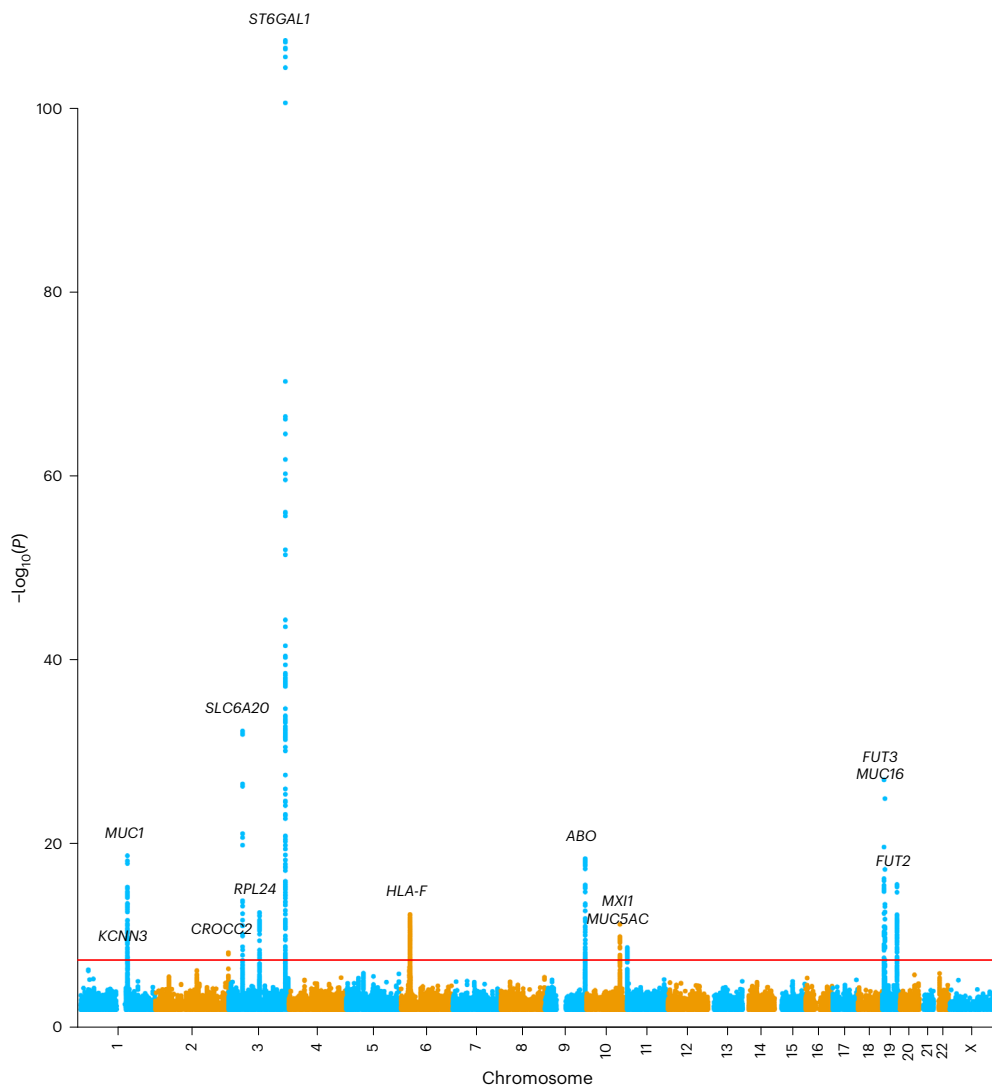


**Fig. 1 | Manhattan plot for GWAS of Omicron infection versus no known infection.** Meta-analysis of four GWAS with a total of 151,825 cases and 556,568 controls under an inverse-variance-weighted fixed-effects model. The y axis shows  $-\log_{10}(P)$  values (two-sided, no adjustment for multiple testing) for SNPs

with  $P < 0.01$  over the chromosomes listed on the x axis. The red line indicates the threshold for genome-wide significance ( $P = 5 \times 10^{-8}$ ), and genome-wide significant loci are annotated with nearby genes.

to the pathway 'entry defense in airway mucus' (nearby genes *MUC1* and *MUC16*) and one to 'viral entry and innate immunity' (*SLC6A20*)<sup>2</sup>. The other two loci previously reported in the context of earlier variants identified in our meta-analysis were represented by [rs13100262](#) (*RPL24*) and [rs492602](#) (*FUT2*). The protective allele [rs492602](#)-G is related to non-secretor status, which confers resistance to childhood ear infection and certain specific viral infections (for example, norovirus, rotavirus), as well as susceptibility to other conditions (for example, mumps, measles, kidney disease)<sup>4,5</sup>.

The most significant finding was the intronic SNP [rs13322149](#) (odds ratio (OR) for minor allele T: 0.857,  $P = 5 \times 10^{-108}$ ) in *ST6GAL1* (ST6 beta-galactoside alpha-2,6-sialyltransferase 1), a gene affecting immune development and function<sup>6</sup>. The encoded protein adds terminal  $\alpha$ 2,6-sialic acids to galactose-containing N-linked glycans. A recent multi-ancestry GWAS of influenza infection also identified a protective effect for the minor allele T<sup>7</sup>. The strong association with influenza was further seen in genome-wide association results from the most recent FinnGen cohort (FinnGen release 12 (<https://www.finngen.fi/en>)), with an OR of 0.889 for [rs13322149](#)-T ( $P = 5.2 \times 10^{-10}$ , 11,558 cases vs 415,538 controls,  $r^2 = 0.965$  between [rs13322149](#) and the FinnGen influenza lead SNP, [rs55958900](#)). The second new locus was represented

by [rs708686](#) (OR for allele T: 1.055,  $P = 1.1 \times 10^{-27}$ ), located intergenic between the fucosyltransferases *FUT6* and *FUT3* (Lewis gene) and from the same gene family as *FUT2*, harboring [rs492602](#) mentioned above. In FinnGen release 12, the risk allele for Omicron infection [rs708686](#)-T was reported as lead SNP in cholelithiasis (OR = 1.103,  $P = 9.6 \times 10^{-41}$ , 49,834 cases vs 437,418 controls), as well as in viral and other specified intestinal infections (OR = 0.913,  $P = 4.4 \times 10^{-10}$ , 11,050 cases vs 444,292 controls), and it was the strongest protein quantitative trait locus (QTL) for *FUT3* levels ( $\beta = -0.657$ ,  $P = 3 \times 10^{-126}$ ) in a proteomics study<sup>8</sup>. The third SNP, [rs10787225](#) (OR for C: 0.966,  $P = 5.3 \times 10^{-12}$ ), is located about 3 kb upstream of *MXI1* (MAX interactor 1), a region with GWAS findings for, among others, blood pressure<sup>9</sup> and blood cell phenotypes<sup>10</sup>, but the previously identified SNPs are not in linkage disequilibrium (LD) with our lead SNP. Additional novel associations include [rs4447600](#) (OR for T: 0.971,  $P = 6.3 \times 10^{-9}$ ) on 2q37.3, which is in moderate LD with [rs6437219](#) ( $r^2 = 0.64$  in the Danish study population), associated with forced vital capacity<sup>11</sup>. Reduced forced vital capacity can indicate reduced lung function, and at this locus, the allele linked to reduced forced vital capacity is in phase with the allele conferring an increased risk of Omicron infection. The genetic association at the *ABO* locus changed drastically, as the previously reported SNP [rs505922](#) linked to

**Table 1 | Associated loci from the meta-analysis**

SNP	Chr	bp (build 38)	Nearby gene	Novel	Ref	Alt	Frequency Alt	OR Alt	Pvalue	Direction	$I^2$	Heterogeneity P
rs1218577	1	154,838,207	KCNN3	Yes	T	C	0.400	0.974	$3.0 \times 10^{-8}$	---+	42.9	0.154
rs6676150	1	155,151,361	MUC1	No	G	C	0.400	1.043	$1.8 \times 10^{-19}$	++++	0	0.526
rs4447600	2	240,905,980	CROCC2	Yes	C	T	0.724	0.971	$6.3 \times 10^{-9}$	---	54.9	0.084
rs9852457	3	45,793,584	SLC6A20	No	G	A	0.066	1.116	$5.3 \times 10^{-33}$	++++	52.7	0.096
rs13100262	3	101,695,258	RPL24	No	T	C	0.354	0.965	$2.7 \times 10^{-13}$	---?	31.6	0.232
rs13322149	3	186,977,425	ST6GAL1	Yes	G	T	0.135	0.857	$5.0 \times 10^{-108}$	---	88.7	$7.1 \times 10^{-6}$
rs34959151	6	29,753,587	HLA-F	Yes	T	TAC	0.756	1.042	$4.5 \times 10^{-13}$	+++?	0	0.4735
rs8176741	9	133,256,074	ABO	Yes	G	A	0.141	0.942	$3.8 \times 10^{-19}$	---	44.3	0.145
rs10787225	10	110,204,375	MXI1	Yes	T	C	0.297	0.966	$5.3 \times 10^{-12}$	---	0	0.794
rs28415845	11	1,151,933	MUC5AC	Yes	T	C	0.689	0.970	$1.8 \times 10^{-9}$	---	27.3	0.248
rs708686	19	5,840,608	FUT3	Yes	C	T	0.326	1.055	$1.1 \times 10^{-27}$	++++	70.4	0.017
rs11673136	19	8,897,072	MUC16	No	A	G	0.459	1.052	$1.1 \times 10^{-25}$	+++?	87.6	$3.2 \times 10^{-4}$
rs492602	19	48,703,160	FUT2	No	A	G	0.383	0.962	$2.5 \times 10^{-16}$	---	77.8	$3.6 \times 10^{-3}$

Results from the meta-analysis of four GWAS with a total of 151,825 cases and 556,568 controls under an inverse-variance-weighted fixed-effects model. P-values are two-sided, not adjusted for multiple testing. Novel column indicates whether loci were novel (yes) or reported to be associated with infections with earlier SARS-CoV-2 variants<sup>2</sup> (no). Frequencies and ORs are shown for the alternative (Alt) allele. The order of the studies in the direction column is according to effective sample size: FinnGen, EstBB, Denmark and MGB Biobank. Heterogeneity was tested with the  $I^2$  statistic and Cochran's Q-test for heterogeneity.

a protective effect of blood group O for earlier variants<sup>2</sup> has changed direction of effect and no longer showed the strongest association (OR for major allele T: 1.022,  $P = 4.8 \times 10^{-6}$ ). Instead, rs8176741 (OR for minor allele A: 0.942,  $P = 3.8 \times 10^{-19}$ ,  $I^2 = 0.159$  with rs505922 in individuals of European ancestry) was the lead SNP, and as it tags blood group B, a protective effect of blood group B against SARS-CoV-2 infection with Omicron variants can be inferred.

The human leukocyte antigen (HLA) region and the MUC5AC locus have previously shown association with COVID-19 severity<sup>2</sup>, but with SNPs that show no strong LD to the lead SNP in this GWAS ( $r^2 < 0.3$ ). Our top HLA SNP, rs34959151 (OR for TAC: 1.042,  $P = 4.5 \times 10^{-13}$ ), is in strong LD with rs1736924 ( $r^2 = 0.989$  in the Danish study population), which tags HLA-F\*01:03 (ref. 12), and there is growing evidence that HLA-F has an important role in immune modulation and viral infection<sup>13</sup>.

Our finding near MUC5AC (rs28415845, OR for C: 0.97,  $P = 1.8 \times 10^{-9}$ ) adds further evidence for the role of mucins in protecting against infection with Omicron variants<sup>14</sup>. Finally, rs1218577 (OR for C: 0.974,  $P = 3 \times 10^{-8}$ ) is located near KCNN3, not far from the MUC1 locus. However, the SNP is located more than 300 kb away from rs6676150 in a different LD block ( $D' = 0.162$ ,  $r^2 = 0.0096$ ) and deserves further attention. Four lead SNPs showed signs of heterogeneity of effect between the study cohorts, with  $P < 0.05$  in Cochran's Q-test and  $I^2 > 60$ . However, all four SNPs have P values well below the genome-wide significance threshold, and the heterogeneity is mainly a result of substantially stronger effect estimates in the Danish cohort (see Supplementary Fig. 2 for forest plots of these four SNPs and Supplementary Table 1 for results of the 13 lead SNPs in all four cohorts). This is probably a consequence of Denmark being one of the countries that had extremely high test activity with easily accessible testing for the whole population<sup>15</sup>; all cases in the cohort were identified by a positive PCR test, and controls were selected based on a negative PCR test and a test history without any positive test.

### Relation to GWAS of earlier SARS-CoV-2 variants

We looked up all 51 SNPs reported by the HGI (in their Supplementary Table S1)<sup>2</sup> as associated with SARS-CoV-2 infection and/or hospitalization (Supplementary Table 2). Apart from the five HGI loci reaching genome-wide significance (Table 1), we observed a comparable effect for rs190509934 close to ACE2, with  $P = 8.9 \times 10^{-7}$  in the FinnGen cohort, indicating that this relatively rare SNP did not

reach genome-wide significance in our study owing to reduced power resulting from being reported in only one cohort. Among the 35 HGI loci with an assigned impact of disease severity (hospitalization), only the one in the HLA region reached genome-wide significance in our GWAS (Supplementary Table 2), but SNP rs2517723 is not in strong LD with our top SNP in the region ( $r^2 < 0.3$ ). This finding is in line with the fact that none of the severity SNPs reached genome-wide significance in the HGI GWAS of infection, even though most of the 49,033 hospitalized cases were also among the 219,692 analyzed cases with infection.

To overcome the problems inherent in comparing two GWAS meta-analyses on different phenotypes and with different cohorts, we investigated differences between the genetic findings for earlier and Omicron variants by performing a second GWAS in our cohorts. Again, we used cases of SARS-CoV-2 infection with Omicron variants, but now versus controls with a SARS-CoV-2 infection before Omicron variants had notable case numbers ('earlier variants'; that is, infection before December 2021,  $n = 87,212$ ). The results we obtained for the lead SNPs from Table 1 (Supplementary Table 3) underlined the emergence of the ST6GAL1 locus ( $P = 2 \times 10^{-49}$ ) and the new lead SNP at the ABO locus ( $P = 1.6 \times 10^{-18}$ ). The difference for the previously reported ABO SNP rs505922 was even larger ( $P = 1.7 \times 10^{-30}$ ), confirming the protective effect observed in earlier variants. For the other lead SNPs, P values ranged from  $9.4 \times 10^{-7}$  to 0.82, with the most significant difference caused by a stronger effect related to Omicron variants at the previously reported MUC16 locus.

### Relation to GWAS of breakthrough infections

A recent GWAS of SARS-CoV-2 breakthrough infections in the UK Biobank identified ten loci<sup>16</sup>, of which eight overlap with our findings (Supplementary Table 4), including all five loci that were also in common with the GWAS of infection with earlier SARS-CoV-2 variants. Among the remaining five loci associated with Omicron infection in our study, lead SNPs at four loci had  $P < 0.001$  in the GWAS of breakthrough infections; only for the secondary signal at the chromosome 1 locus, there was no sign of association. The lead SNPs at the two remaining loci in the GWAS of breakthrough infections had attenuated effect sizes and only reached nominal significance in our meta-analysis. The UK Biobank study did not specify the time period in which the breakthrough infections occurred; however, given the overall large fraction of Omicron infections among all SARS-CoV-2 breakthrough infections,

it can be expected that Omicron accounted for the majority of cases. For Denmark, vaccination data were available, and we compared within the Omicron cases 20,754 individuals with a completed initial round of vaccination versus 1,167 without any vaccination. We observed no significant differences at the adjusted  $P$  value of 0.038 (0.05 / 13) for any of the 13 SNPs in Table 1, and the direction of effect did not consistently agree or disagree with the results in the main GWAS of Omicron cases versus controls (Supplementary Table 5).

### Relation to GWAS of influenza

We looked up our genome-wide significant loci in a recent GWAS of influenza (Supplementary Table 6), a study that also reported [rs13322149](#) near *ST6GAL1* as the lead SNP with a similar effect (OR for T: 0.888,  $P = 3.6 \times 10^{-19}$ )<sup>7</sup>.

In a total of 14 comparisons (including the only other lead SNP, [rs2837113](#), from the influenza GWAS), we observed two more of our loci reaching the adjusted significance level of  $4.2 \times 10^{-3}$  for influenza: [rs6676150](#) (OR for C: 1.038,  $P = 1.1 \times 10^{-6}$ ) and the proxy SNP [rs73005873](#) (OR for C: 1.033,  $P = 5.0 \times 10^{-5}$ ) near *MUC1* and *MUC16*, respectively, with consistent directions of effects between the studies. By contrast, the second lead SNP identified in the influenza GWAS ([rs2837113](#), *B3GALT5* locus, OR for A: 0.915,  $P = 4.1 \times 10^{-32}$ ) went in the opposite direction for Omicron (OR for A: 1.016,  $P = 7.5 \times 10^{-4}$ ). Earlier studies<sup>7,17</sup> have seen some indication for an increased risk of influenza associated with SNPs in LD with the protective *ABO* lead SNP [rs505922](#) from the HGI GWAS of earlier SARS-CoV-2 variants<sup>2</sup>. However, the lead SNP at the *ABO* locus in our GWAS shows no sign of association in the influenza GWAS ( $P = 0.215$ ).

### Open Targets Genetics analysis

To investigate connections between the 13 GWAS loci and genes based on extensive data from gene expression, protein abundance and chromatin interaction, we put the 13 lead SNPs forward to Open Targets Genetics<sup>18</sup> (<https://genetics.opentargets.org>; accession date: 20 January 2025). The summary statistics from the variant-to-gene (V2G) analysis are given in Supplementary Table 7. For *ABO* and *FUT3*, relatively large V2G scores (0.47 and 0.34, respectively) were observed, while no other gene at the loci had a V2G score of  $>0.2$ . Gene connections were also observed for the SNPs at the other loci, but the V2G scores did not clearly favor single genes at those loci.

### Gene-set and pathway analysis

We followed up on our GWAS with FUMA (v.1.5.2)<sup>19</sup> for a comprehensive integration of our results with public resources, including functional annotation, expression QTL and chromatin interaction mapping, as well as additional gene-based, pathway and tissue enrichment tests (for full results, see <https://fuma.ctglab.nl/browse/475677>). To answer whether other traits or diseases are associated with the identified SNPs for Omicron infection, FUMA provides entries from the GWAS Catalog for SNPs in LD with the lead SNPs.

In addition, we performed a comprehensive genome-wide association study in 2,470 phenotypes available in FinnGen release 12 for the lead SNPs (Supplementary Table 8), in which the posterior inclusion probability, calculated with SuSiE<sup>20</sup>, indicates whether our lead SNP is causal for the observed phenotype association.

The MAGMA (v.1.08)<sup>21</sup> gene-set analysis (<https://fuma.ctglab.nl/browse/475677>) identified the Reactome set 'Termination of O-glycan biosynthesis' as the top set among a variety of 17,012 gene sets ( $P = 6.8 \times 10^{-7}$ ). Among the 23 genes in this gene set are *ST6GAL1* and several mucin genes, including *MUC1*, *MUC5AC* and *MUC16*, located in three distinct genome-wide significant loci in our study. The finding proved to be robust in a sensitivity analysis, leaving one of these four loci out at a time (see section 'MAGMA gene-set sensitivity analysis' in the Supplementary Note). FUMA provides the secondary analysis process, GENE2FUNC, to further investigate biological mechanisms of

prioritized genes. Running GENE2FUNC for the 65 positional candidate genes from the SNP2GENE analysis, ten Reactome gene sets with an adjusted  $P < 0.05$  were identified, eight of which are related to mucins or glycosylation (Supplementary Table 9).

### Functional protein association network analysis

To find further evidence for a relevant role of genes at the identified genomic loci, we conducted a functional protein association network analysis. This approach allows for the contextualization and visualization of significant pathways while also revealing additional functional connections between proteins. To avoid retrieving associations driven solely by genes located at the same locus, we started by selecting one gene for each of our 13 GWAS loci. The resulting network has a protein–protein interaction enrichment  $P$  value of  $1.33 \times 10^{-11}$ , indicating that these 13 proteins are at least partially biologically connected as a functional group. Seven of the 13 proteins had functional associations above the default medium confidence score threshold of 0.4, and *MUC1*, *MUC16* and *MUC5AC* also interacted physically in addition to their functional associations (Fig. 2a). As mentioned above, *ST6GAL1* and the three mucins are all involved in the Reactome<sup>22</sup> pathway 'Termination of O-glycan biosynthesis', in which *ST6GAL1* transfers sialic acid to galactose-containing acceptor substrates (here the mucins), and the connections were mainly a result of their involvement in this pathway. The connected component in this network also included *FUT2*, *FUT3* and *ABO*, with the significant functional enrichment resulting from their involvement in the KEGG<sup>23</sup> pathway 'Glycosphingolipid biosynthesis—lacto and neolacto series' (the only significant pathway in the specific analysis for KEGG gene sets in the secondary MAGMA analysis GENE2FUNC; adjusted  $P = 2.2 \times 10^{-4}$ ). In addition to these well-established connections, there were some weaker associations between *ST6GAL1*, *FUT2* and *FUT3*, as well as between *FUT3* and *MUC1*. The former connections were a result of these proteins regulating glycosylation processes<sup>24,25</sup>, while the association between *FUT3* and *MUC1* was observed in aberrant glycosylation processes<sup>24</sup>. We expanded the network with 15 additional interactors at a maximum selectivity value of 1 to focus on proteins that primarily interact with the current network. For four of the identified interactors, the corresponding gene was in a genomic locus already covered. The resulting highly specific network (Fig. 2b) showed that the expansion added more proteins to the pathways already identified above and has a protein–protein interaction enrichment  $P$  value  $< 10^{-16}$ . Among the added proteins, another sialyltransferase (*ST3GAL4*) was involved in both pathways and represents a strong link between the two sets of proteins.

### Heritability and genetic correlations

We estimated heritability from our GWAS at the liability scale, assuming a prevalence of 0.5, as 0.024 (95% CI, 0.018–0.029), slightly higher than the heritability estimates for the HGI GWAS of infection versus population controls in European ancestry (estimates for different scenarios were all below 0.019)<sup>2</sup>.

The genetic correlation between our GWAS for infection with Omicron variants and the publicly available meta-analysis results for infection with earlier variants from the HGI for individuals of European ancestry was estimated as  $r_g = 0.549$  (95% CI, 0.342–0.757,  $P = 2.06 \times 10^{-7}$ ). We also investigated genetic correlations of our GWAS with GWAS for 1,461 traits implemented in the Complex Traits Genetics Virtual Lab (<https://vl.genoma.io>), with most results coming from the UK Biobank. With schizophrenia,  $r_g = -0.265$  (95% CI, -0.347 to -0.182,  $P = 2.95 \times 10^{-10}$ ), and asthma,  $r_g = 0.289$  (95% CI, 0.187–0.390,  $P = 2.67 \times 10^{-8}$ ), two serious health conditions were among the traits reaching the adjusted significance level of  $3.4 \times 10^{-5}$  (Supplementary Table 10). We further investigated these genetic correlations with bivariate Gaussian mixture models implemented in MiXeR<sup>26</sup> (v.1.3), but the model fit was poor compared to the LD score regression model (see section 'MiXeR analyses of GWAS for infection

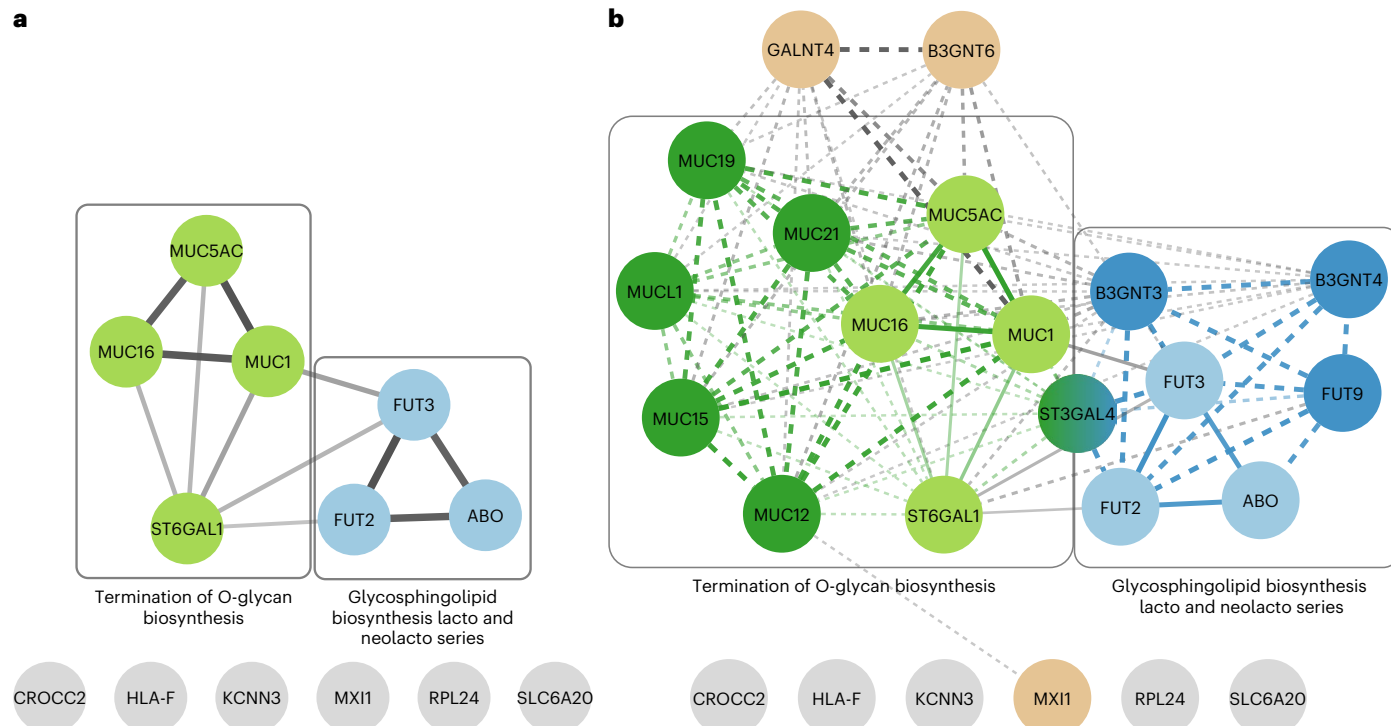


**Fig. 2 | STRING networks.** **a**, STRING network for 13 genes linked to the GWAS lead SNPs. Proteins involved in the ‘Termination of O-glycan biosynthesis’ pathway are colored light green, while proteins involved in ‘Glycosphingolipid biosynthesis—lacto and neolacto series’ are colored light blue. The two sets of proteins form a connected component, with ST6GAL1 and FUT3 acting as the main bridges. The edge width is indicative of the confidence score for each association, with thicker edges denoting higher confidence scores. Proteins with no interactions are colored light gray. The resulting network can be viewed, explored and customized at <https://version-12.0.string-db.org/cgi/network?networkId=bn0f0k57q9qc>. **b**, STRING network expanded with 15 additional interactors using a selectivity parameter of 1.0. Four interactors were removed because the corresponding genes were located in genomic loci already covered (FUT5, FUT6, MUC22, MUC3A). Additional proteins that belong to the ‘Termination of O-glycan biosynthesis’ pathway are

shown in dark green, and additional proteins that belong to the ‘Glycosphingolipid biosynthesis—lacto and neolacto series’ pathway are shown in dark blue. Additional connected proteins not belonging to either of the two pathways are shown in beige. The addition of the extra proteins leads to a heavily interconnected network; for this reason, we have selected a special coloring scheme to distinguish between the different edges in the network. Solid lines represent associations between the 13 original genes and dashed lines represent associations from the 11 additional genes. Green edges show associations between the genes involved in the ‘Termination of O-glycan biosynthesis’ pathway, blue edges show associations between the genes involved in the ‘Glycosphingolipid biosynthesis—lacto and neolacto series’ pathway, and gray lines represent other associations. This network can also be accessed at <https://version-12.0.string-db.org/cgi/network?networkId=bTU3KlbwyQXZ>. The data underlying these networks are provided as source data.

with Omicron variants and GWAS for ‘schizophrenia and asthma’ in the Supplementary Note). Finally, we looked up the lead SNPs from Table 1 in the GWAS of schizophrenia<sup>27</sup> and asthma<sup>28</sup> (Supplementary Tables 11 and 12, respectively). For asthma, two SNPs at mucin loci (*MUC5AC* and *MUC16*) show *P* values below the adjusted *P* value of 0.0038 (0.05/13) and agree with the top asthma SNPs at the loci. Contrary to the positive genetic correlation estimated over the whole genome, the two mucin genes have asthma ORs in the opposite direction to the Omicron infection GWAS.

## Discussion

We performed a GWAS of SARS-CoV-2 infection with Omicron variants in >150,000 cases and >500,000 controls without a known SARS-CoV-2 infection from four cohorts of European ancestry and identified 13 genome-wide significant loci. The restriction to European ancestry limits the generalizability of our findings, and it will be important to study SARS-CoV-2 infection with Omicron variants at a considerable sample size in other parts of the world. Our study investigated infection during the Omicron period in general, given that information on the sub-variants of Omicron that regularly emerge was not available at an individual level. However, more than 70% of our cases were from the first 6 months of 2022, when BA variants were dominating in the study populations (see Supplementary Figs. 3 and 4). Notably, our findings are corroborated by a recent GWAS of breakthrough infections<sup>16</sup>, probably dominated by Omicron infections. Breakthrough and Omicron

infections are closely related in large parts of Europe and the USA, as the extensive vaccination programs rolled out in 2021 exerted strong selective pressure on the SARS-CoV-2 virus and were followed by the evolution and rapid spread of Omicron variants.

Among our findings, the most significant SNP is an intronic transversion mutation ([rs13322149](https://www.ncbi.nlm.nih.gov/snp/rs13322149): G > T) located within the 148 kb *ST6GAL1* gene. *ST6GAL1* catalyzes the addition of terminal α2,6-sialic acids to galactose-containing N-linked glycans and is highly expressed in the liver, glandular cells in the prostate, collecting ducts and distal tubules in the kidneys and germinal centers in lymph nodes (<https://www.proteinatlas.org/ENSG00000073849-ST6GAL1/tissue>). Expression of *ST6GAL1* also enhances the concentration of six-linked sialic acid receptors that are accessible to the influenza virus on the cell surface<sup>29</sup>. Based on knowledge from other coronaviruses (including MERS-CoV recognizing α2,3-sialic acids and, to a lesser extent, the α2,6-sialic acids and sulfated sialyl-Lewis<sup>X</sup> for binding preference), a role of O-acetylated sialic acids in the entry of SARS-CoV-2 into the host cell was postulated early in the pandemic<sup>30</sup>, resulting in multiple studies on the topic in a short time<sup>31</sup>.

It is evident from *in vitro* and *in vivo* studies that the emergence of Omicron changed the interaction of SARS-CoV-2 with the host. Compared to the ancestral B.1. lineage virus and the Delta variant, Omicron viral entry and infection is significantly attenuated in immortalized lung cell lines<sup>32–34</sup> and human-derived lung organoids<sup>35</sup> but increased in human-derived upper airway organoids<sup>32</sup>. In transgenic mice and

Syrian hamsters, Omicron is also less pathogenic, with reduced infection and pathology in the lower airways<sup>36</sup> but with greater affinity for tracheal cells<sup>37</sup>. The mechanism underlying this tropism shift is not fully understood. Here, the association of our *ST6GAL1* SNP rs1334922 with reduced infection risk for Omicron but not pre-Omicron variants suggests an involvement of α2,6-sialic acids that emerged with the evolution of this SARS-CoV-2 variant. Considering that the same *ST6GAL1* lead SNP is protective against influenza infection, a virus that enters cells through binding α2,6-sialic acids, and the dependency of other beta coronaviruses on sialic acids for host cell entry (reviewed in a previous work<sup>31</sup>) warrants a re-evaluation of the role of sialic acids in SARS-CoV-2 host cell entry for Omicron variants.

In addition to a role for host cell glycosylation in viral entry, the SARS-CoV-2 spike protein is itself heavily glycosylated, with 22 N-glycosylation sites per monomer. These glycans shield the protein from the host's humoral immune response<sup>38,39</sup> and are generally conserved across earlier and later variants, including Omicron<sup>40,41</sup>. However, Omicron has decreased sialylation of these glycans<sup>40,42</sup>, which is speculated to reduce electrostatic repulsion and steric hindrance when binding to the ACE2 receptor and ultimately promote stronger binding between the Omicron spike and this host receptor<sup>43,44</sup>. Glycosylation near the furin cleavage site can also regulate viral activity<sup>45,46</sup>, whereby sialic acid occupancy on O-glycans decreases furin activity by up to 65% (ref. 47). Together, these results suggest that a reduction in sialic acid levels on the spike protein can enhance the infectivity of SARS-CoV-2 through improved binding to the ACE2 receptor and increased furin activity.

Gene-set analysis linked *ST6GAL1* to mucin genes, and our GWAS identified three loci with mucin candidate genes (*MUC1*, *MUC5AC* and *MUC16*), showing that the biological pathway of airway defense in mucus, linked to infections with earlier SARS-CoV-2 variants<sup>2</sup>, also has an important role in relation to Omicron variants. A recent GWAS of influenza identified two SNPs associated at genome-wide significance and, based on SARS-CoV-2 GWAS results for earlier variants, concluded that the genetic architectures of COVID-19 and influenza are mostly distinct. Our results provide nuance, as our *ST6GAL1* SNP for Omicron infection was one of the two lead SNPs for influenza infection and showed a similar effect. Additionally, two of our three mucin loci had suggestive findings in the influenza GWAS.

Additional evidence for a connection between blood group systems and SARS-CoV-2 infection was obtained by three associated loci, finding the same association at the *FUT2* locus determining secretor status as described for earlier variants, identifying a new locus near *FUT3* and observing substantial differences at the *ABO* locus, where the lead SNP indicates a protective effect of blood group B. All three loci encode glycosyltransferases involved in forming blood group antigens on red blood cells, tissues and in secretions (see section 'Discussion of the role of blood group systems in infection' in the Supplementary Note for a discussion of the role of blood group systems in infection and the related Supplementary Fig. 5, showing ABO and Lewis blood group antigen synthesis). We want to stress that our results did not contradict the protective effect of blood group O reported for earlier variants, as the previously associated SNP was the one showing the largest difference between cases infected with Omicron variants versus controls infected with earlier variants. Furthermore, there have been association findings for several other infectious diseases at the *ABO* locus, as summarized in a recent influenza study<sup>7</sup>. None of the lead SNPs reported there for influenza, malaria, tonsillectomy, childhood ear infection or gastrointestinal infection are in LD with our lead SNP, rs8176741.

In conclusion, our study indicates that the human genetic architecture of SARS-CoV-2 infection is under constant development, and updated GWAS analyses for periods during which certain variants dominate can provide further insights into the biological mechanisms involved. Our results indicate that processes related to glycosylation

are particularly relevant for infections with Omicron variants. Experimental studies comparing the infectivity of different SARS-CoV-2 variants in relation to host cell expression of *ST6GAL1* and other mediators of glycosylation are needed to decipher the underlying biology.

## Online content

Any methods, additional references, Nature Portfolio reporting summaries, source data, extended data, supplementary information, acknowledgements, peer review information; details of author contributions and competing interests; and statements of data and code availability are available at <https://doi.org/10.1038/s41588-025-02484-9>.

## References

1. World Health Organization. COVID-19 cases. WHO COVID-19 dashboard. <https://data.who.int/dashboards/covid19/cases> (2025).
2. Kanai, M. et al. A second update on mapping the human genetic architecture of COVID-19. *Nature* **621**, E7–E26 (2023).
3. Markov, P. V. et al. The evolution of SARS-CoV-2. *Nat. Rev. Microbiol.* **21**, 361–379 (2023).
4. Azad, M. B., Wade, K. H. & Timpton, N. J. *FUT2* secretor genotype and susceptibility to infections and chronic conditions in the ALSPAC cohort. *Wellcome Open Res.* **3**, 65 (2018).
5. Tian, C. et al. Genome-wide association and HLA region fine-mapping studies identify susceptibility loci for multiple common infections. *Nat. Commun.* **8**, 599 (2017).
6. Jones, M. B. IgG and leukocytes: targets of immunomodulatory α2,6 sialic acids. *Cell. Immunol.* **333**, 58–64 (2018).
7. Kosmicki, J. A. et al. Genetic risk factors for COVID-19 and influenza are largely distinct. *Nat. Genet.* **56**, 1592–1596 (2024).
8. Emilsson, V. et al. Co-regulatory networks of human serum proteins link genetics to disease. *Science* **361**, 769–773 (2018).
9. Keaton, J. M. et al. Genome-wide analysis in over 1 million individuals of European ancestry yields improved polygenic risk scores for blood pressure traits. *Nat. Genet.* **56**, 778–791 (2024).
10. Sakaue, S. et al. A cross-population atlas of genetic associations for 220 human phenotypes. *Nat. Genet.* **53**, 1415–1424 (2021).
11. Shrine, N. et al. New genetic signals for lung function highlight pathways and chronic obstructive pulmonary disease associations across multiple ancestries. *Nat. Genet.* **51**, 481–493 (2019).
12. Paganini, J. et al. HLA-F transcriptional and protein differential expression according to its genetic polymorphisms. *HLA* **102**, 578–589 (2023).
13. Lin, A. & Yan, W. H. The emerging roles of human leukocyte antigen-F in immune modulation and viral infection. *Front. Immunol.* **10**, 449250 (2019).
14. Noh, H. E. & Rha, M. S. Mucosal immunity against SARS-CoV-2 in the respiratory tract. *Pathogens* **13**, 113 (2024).
15. Gram, M. A. et al. Patterns of testing in the extensive Danish national SARS-CoV-2 test set-up. *PLoS ONE* **18**, e0281972 (2023).
16. Alcalde-Herraiz, M. et al. Genome-wide association studies of COVID-19 vaccine seroconversion and breakthrough outcomes in UK Biobank. *Nat. Commun.* **15**, 8739 (2024).
17. Shelton, J. F. et al. Trans-ancestry analysis reveals genetic and nongenetic associations with COVID-19 susceptibility and severity. *Nat. Genet.* **53**, 801–808 (2021).
18. Ghoussaini, M. et al. Open Targets Genetics: systematic identification of trait-associated genes using large-scale genetics and functional genomics. *Nucleic Acids Res.* **49**, D1311–D1320 (2021).
19. Watanabe, K., Taskesen, E., van Bochoven, A. & Posthuma, D. Functional mapping and annotation of genetic associations with FUMA. *Nat. Commun.* **8**, 1826 (2017).

20. Wang, G., Sarkar, A., Carbonetto, P. & Stephens, M. A simple new approach to variable selection in regression, with application to genetic fine mapping. *J. R. Stat. Soc. Series B Stat. Methodol.* **82**, 1273–1300 (2020).

21. de Leeuw, C. A., Mooij, J. M., Heskes, T. & Posthuma, D. MAGMA: generalized gene-set analysis of GWAS data. *PLoS Comput. Biol.* **11**, e1004219 (2015).

22. Milacic, M. et al. The Reactome Pathway Knowledgebase 2024. *Nucleic Acids Res.* **52**, D672–D678 (2024).

23. Kanehisa, M., Goto, S., Sato, Y., Furumichi, M. & Tanabe, M. KEGG for integration and interpretation of large-scale molecular data sets. *Nucleic Acids Res.* **40**, D109–D114 (2012).

24. Fernández-Ponce, C. et al. The role of glycosyltransferases in colorectal cancer. *Int. J. Mol. Sci.* **22**, 5822 (2021).

25. Zhu, J., Dingess, K. A., Mank, M., Stahl, B. & Heck, A. J. R. Personalized profiling reveals donor- and lactation-specific trends in the human milk proteome and peptidome. *J. Nutr.* **151**, 826–839 (2021).

26. Frei, O. et al. Bivariate causal mixture model quantifies polygenic overlap between complex traits beyond genetic correlation. *Nat. Commun.* **10**, 2417 (2019).

27. Ripke, S. et al. Biological insights from 108 schizophrenia-associated genetic loci. *Nature* **511**, 421–427 (2014).

28. Zhou, W. et al. Global Biobank Meta-analysis Initiative: powering genetic discovery across human disease. *Cell Genomics* **2**, 100192 (2022).

29. Matrosovich, M., Matrosovich, T., Carr, J., Roberts, N. A. & Klenk, H.-D. Overexpression of the α-2,6-sialyltransferase in MDCK cells increases influenza virus sensitivity to neuraminidase inhibitors. *J. Virol.* **77**, 8418 (2003).

30. Kim, C. H. SARS-CoV-2 evolutionary adaptation toward host entry and recognition of receptor O-acetyl sialylation in virus–host interaction. *Int. J. Mol. Sci.* **21**, 4549 (2020).

31. Sun, X. L. The role of cell surface sialic acids for SARS-CoV-2 infection. *Glycobiology* **31**, 1245–1253 (2021).

32. Mykytyn, A. Z. et al. SARS-CoV-2 Omicron entry is type II transmembrane serine protease-mediated in human airway and intestinal organoid models. *J. Virol.* **97**, e0085123 (2023).

33. Willett, B. J. et al. SARS-CoV-2 Omicron is an immune escape variant with an altered cell entry pathway. *Nat. Microbiol.* **7**, 1161–1179 (2022).

34. Laine, L., Skön, M., Väistönen, E., Julkunen, I. & Österlund, P. SARS-CoV-2 variants Alpha, Beta, Delta and Omicron show a slower host cell interferon response compared to an early pandemic variant. *Front. Immunol.* **13**, 1016108 (2022).

35. Flagg, M. et al. Low level of tonic interferon signalling is associated with enhanced susceptibility to SARS-CoV-2 variants of concern in human lung organoids. *Emerg. Microbes Infect.* **12**, 2276338 (2023).

36. Halfmann, P. J. et al. SARS-CoV-2 Omicron virus causes attenuated disease in mice and hamsters. *Nature* **603**, 687–692 (2022).

37. Armando, F. et al. SARS-CoV-2 Omicron variant causes mild pathology in the upper and lower respiratory tract of hamsters. *Nat. Commun.* **13**, 3519 (2022).

38. Watanabe, Y., Bowden, T. A., Wilson, I. A. & Crispin, M. Exploitation of glycosylation in enveloped virus pathobiology. *Biochim. Biophys. Acta Gen. Subj.* **1863**, 1480–1497 (2019).

39. Casalino, L. et al. Beyond shielding: the roles of glycans in the SARS-CoV-2 spike protein. *ACS Cent. Sci.* **6**, 1722–1734 (2020).

40. Shahajan, A., Pepi, L. E., Kumar, B., Murray, N. B. & Azadi, P. Site specific N- and O-glycosylation mapping of the spike proteins of SARS-CoV-2 variants of concern. *Sci. Rep.* **13**, 10053 (2023).

41. Wang, D. et al. Enhanced surface accessibility of SARS-CoV-2 Omicron spike protein due to an altered glycosylation profile. *ACS Infect. Dis.* **13**, 23 (2024).

42. Xie, Y. & Butler, M. Quantitative profiling of N-glycosylation of SARS-CoV-2 spike protein variants. *Glycobiology* **33**, 188–202 (2023).

43. Huang, C. et al. The effect of N-glycosylation of SARS-CoV-2 spike protein on the virus interaction with the host cell ACE2 receptor. *iScience* **24**, 103272 (2021).

44. Zheng, L. et al. Characterization and function of glycans on the spike proteins of SARS-CoV-2 variants of concern. *Microbiol. Spectr.* **10**, e0312022 (2022).

45. Wang, S. et al. Sequential glycosylations at the multibasic cleavage site of SARS-CoV-2 spike protein regulate viral activity. *Nat. Commun.* **15**, 4162 (2024).

46. Zhang, L. et al. Furin cleavage of the SARS-CoV-2 spike is modulated by O-glycosylation. *Proc. Natl Acad. Sci. USA* **118**, e2109905118 (2021).

47. Gonzalez-Rodriguez, E. et al. O-Linked sialoglycans modulate the proteolysis of SARS-CoV-2 spike and likely contribute to the mutational trajectory in variants of concern. *ACS Cent. Sci.* **9**, 393–404 (2023).

**Publisher's note** Springer Nature remains neutral with regard to jurisdictional claims in published maps and institutional affiliations.

**Open Access** This article is licensed under a Creative Commons Attribution-NonCommercial-NoDerivatives 4.0 International License, which permits any non-commercial use, sharing, distribution and reproduction in any medium or format, as long as you give appropriate credit to the original author(s) and the source, provide a link to the Creative Commons licence, and indicate if you modified the licensed material. You do not have permission under this licence to share adapted material derived from this article or parts of it. The images or other third party material in this article are included in the article's Creative Commons licence, unless indicated otherwise in a credit line to the material. If material is not included in the article's Creative Commons licence and your intended use is not permitted by statutory regulation or exceeds the permitted use, you will need to obtain permission directly from the copyright holder. To view a copy of this licence, visit <http://creativecommons.org/licenses/by-nc-nd/4.0/>.

© The Author(s) 2026

**Frank Geller**  , **Xiaoping Wu**  , **Vilma Lammi**  , **Erik Abner**  , **Jesse Tyler Valliere**  , **Katerina Nastou**<sup>1</sup>, **Angus Burns**  , **Morten Rasmussen**<sup>8</sup>, **Niklas Worm Andersson**  , **DBDS Genomic Consortium**<sup>\*</sup>, **Bitten Aagaard**  , **Karina Banasik**<sup>11,12</sup>, **Sofie Bliddal**  , **Lasse Boding**<sup>14</sup>, **Søren Brunak**  , **Nanna Brøns**<sup>3</sup>, **Jonas Bybjerg-Grauholm**  , **Lea Arregui Nordahl Christoffersen**<sup>9,15</sup>, **Maria Didriksen**  , **Khoa Manh Dinh**  , **Christian Erikstrup**  , **Ulla Feldt-Rasmussen**<sup>13,19</sup>, **Kirsten Grønbæk**  , **Kathrine Agergård Kaspersen**  , **Christina Mikkelsen**  , **Claus Henrik Nielsen**<sup>23</sup>, **Henriette Svarre Nielsen**  , **Susanne Dam Nielsen**<sup>24</sup>, **Janna Nissen**  , **Celia Burgos Sequeros**  , **Niels Tommerup**  , **Henrik Ullum**<sup>26</sup>, **Estonian Biobank Research Team**<sup>\*</sup>, **FinnGen**<sup>\*</sup>, **Lampros Spiliopoulos**<sup>1</sup>, **Peter Bager**<sup>1</sup>, **Anders Hviid**  , **Erik Sørensen**  , **Ole Birger Pedersen**  , **Sisse Rye Ostrowski**   & **Bjarke Feenstra**  <img alt="Email icon" data-bbox="45638 795 4575

<sup>1</sup>Department of Epidemiology Research, Statens Serum Institut, Copenhagen, Denmark. <sup>2</sup>Department of Congenital Disorders, Statens Serum Institut, Copenhagen, Denmark. <sup>3</sup>Department of Clinical Immunology, Rigshospitalet, Copenhagen University Hospital, Copenhagen, Denmark. <sup>4</sup>Institute for Molecular Medicine Finland (FIMM), HiLIFE, University of Helsinki, Helsinki, Finland. <sup>5</sup>Molecular and Population Genetics Program, Broad Institute, Cambridge, MA, USA. <sup>6</sup>Estonian Genome Center, Institute of Genomics, University of Tartu, Tartu, Estonia. <sup>7</sup>Center for Genomic Medicine, Massachusetts General Hospital, Boston, MA, USA. <sup>8</sup>Virus Research and Development Laboratory, Virus & Microbiological Special Diagnostics, Statens Serum Institut, Copenhagen, Denmark. <sup>9</sup>Department of Clinical Immunology, Zealand University Hospital, Køge, Denmark. <sup>10</sup>Department of Clinical Immunology, Aalborg University Hospital, Aalborg, Denmark. <sup>11</sup>Department of Obstetrics and Gynecology, Copenhagen University Hospital, Amager & Hvidovre Hospital, Copenhagen, Denmark. <sup>12</sup>Novo Nordisk Foundation Center for Protein Research, Faculty of Health and Medical Sciences, University of Copenhagen, Copenhagen, Denmark. <sup>13</sup>Department of Nephrology and Endocrinology, Rigshospitalet, Copenhagen University Hospital, Copenhagen, Denmark. <sup>14</sup>Danish National Biobank, Statens Serum Institut, Copenhagen, Denmark. <sup>15</sup>Institute of Biological Psychiatry, Copenhagen Mental Health Services, Copenhagen University Hospital, Copenhagen, Denmark. <sup>16</sup>Department of Neuroscience, Faculty of Health and Medical Sciences, University of Copenhagen, Copenhagen, Denmark. <sup>17</sup>Department of Clinical Immunology, Aarhus University Hospital, Aarhus, Denmark. <sup>18</sup>Department of Clinical Medicine, Aarhus University, Aarhus, Denmark. <sup>19</sup>Department of Clinical Medicine, Faculty of Health and Medical Sciences, University of Copenhagen, Copenhagen, Denmark. <sup>20</sup>Department of Hematology, Rigshospitalet, Copenhagen University Hospital, Copenhagen, Denmark. <sup>21</sup>Biotech Research and Innovation Center (BRIC), University of Copenhagen, Copenhagen, Denmark. <sup>22</sup>Novo Nordisk Center for Basic Metabolic Research, Faculty of Health and Medical Sciences, University of Copenhagen, Copenhagen, Denmark. <sup>23</sup>Institute for Inflammation Research, Center for Rheumatology and Spine Diseases, Rigshospitalet, Copenhagen University Hospital, Copenhagen, Denmark. <sup>24</sup>Viro-Immunology Research Unit, Department of Infectious Diseases, Rigshospitalet, Copenhagen University Hospital, Copenhagen, Denmark. <sup>25</sup>Department of Cellular and Molecular Medicine, Faculty of Health and Medical Sciences, University of Copenhagen, Copenhagen, Denmark. <sup>26</sup>Statens Serum Institut, Copenhagen, Denmark. <sup>27</sup>Pharmacovigilance Research Center, Department of Drug Design and Pharmacology, Faculty of Health and Medical Sciences, University of Copenhagen, Copenhagen, Denmark. <sup>28</sup>Anesthesia, Critical Care, and Pain Medicine, Massachusetts General Hospital and Harvard Medical School, Boston, MA, USA. <sup>29</sup>Department of Biology, University of Copenhagen, Copenhagen, Denmark. <sup>30</sup>These authors jointly supervised this work: Hanna M. Ollila, Sisse Rye Ostrowski, Bjarke Feenstra.

\*A list of authors and their affiliations appears at the end of the paper.  e-mail: [fge@ssi.dk](mailto:fge@ssi.dk)

---

## DBDS Genomic Consortium

**Frank Geller<sup>1,2,3</sup>, Liam Quinn<sup>9</sup>, Karina Banasik<sup>11,12</sup>, Søren Brunak<sup>12</sup>, Lea Arregui Nordahl Christoffersen<sup>9,15</sup>,  
Maria Didriksen<sup>3,16</sup>, Khoa Manh Dinh<sup>3,17</sup>, Christian Erikstrup<sup>17,18</sup>, Kathrine Agergård Kaspersen<sup>17</sup>, Christina Mikkelsen<sup>3,22</sup>,  
Janna Nissen<sup>3</sup>, Henrik Ullum<sup>26</sup>, Erik Sørensen<sup>3</sup>, Ole Birger Pedersen<sup>9,19</sup>, Sisse Rye Ostrowski<sup>3,19,30</sup> &  
Bjarke Feenstra<sup>1,2,3,29,30</sup>**

---

A full list of members and their affiliations appears in the Supplementary Information.

---

## Estonian Biobank Research Team

**Erik Abner<sup>6</sup>**

---

## FinnGen

**Hanna M. Ollila<sup>4,28,30</sup>**

A full list of members and their affiliations appears in the Supplementary Information.

## Methods

### Ethics

Our research complies with all relevant ethical regulations for the cohorts under study.

The Copenhagen Hospital Biobank provides biological leftover samples from routine blood analyses, and the patients were not asked for informed consent before inclusion. Instead, patients were informed about the opt-out option to have their biological specimens excluded from use in research. Individuals from the exclusion register (Vævsanvendelsesregistret) were excluded from the study. For the Danish Blood Donor Study, informed consent was obtained from all participants. Both studies are part of a COVID-19 protocol approved by the National Ethics Committee (H-21030945) and the Danish Data Protection Agency (P-2020-356).

EFTER-COVID was conducted as a surveillance study as part of Statens Serum Institut's advisory tasks for the Danish Ministry of Health. According to Danish law, these national surveillance activities do not require approval from an ethics committee. Participation in the study was voluntary, and the invitation letter contained information about participants' rights under the Danish General Data Protection Regulation (rights to access data, rectification, deletion, restriction of processing and objection). After reading this information, it was considered informed consent when participants read the information and agreed, and then continued to fill in the questionnaires.

The activities of the Estonian Biobank (EstBB) are regulated by the Human Genes Research Act, which was adopted in 2000 specifically for the operations of the EstBB. Individual-level analysis with EstBB data was carried out under ethical approval 1.1-12/624 from the Estonian Committee on Bioethics and Human Research (Estonian Ministry of Social Affairs), using data according to release application 6-7/GI/5933 from the EstBB.

Study participants in FinnGen provided informed consent for biobank research, based on the Finnish Biobank Act. Alternatively, separate research cohorts, collected before the Finnish Biobank Act came into effect (in September 2013) and the start of FinnGen (August 2017), were collected based on study-specific consents and later transferred to the Finnish biobanks after approval by Fimea (Finnish Medicines Agency), the National Supervisory Authority for Welfare and Health. Recruitment protocols followed the biobank protocols approved by Fimea. The Coordinating Ethics Committee of the Hospital District of Helsinki and Uusimaa statement number for the FinnGen study is HUS/990/2017. The FinnGen study is approved by the Finnish Institute for Health and Welfare and other authorities (a complete overview of permissions is given in the Supplementary Data).

The Mass General Brigham (MGB) Biobank, formerly known as the Partners Biobank, is a hospital-based cohort study produced by the MGB healthcare network located in Boston, MA, USA. The MGB Biobank contains data from patients in multiple primary care facilities as well as tertiary care centers located in the greater Boston area. Participants of the study are recruited from inpatient stays, emergency department environments, outpatient visits and through a secure online portal available to patients. Recruitment and consent are fully translatable to Spanish in order to promote greater patient diversity. This allows for a systematic enrollment of diverse patient groups that is reflective of the population receiving care through the MGB network. Recruitment for the biobank began in 2009 and is still actively recruiting. The recruitment strategy has been described previously<sup>48</sup>. For the MGB Biobank, all patients provide written consent upon enrollment. Furthermore, the MGB cohort included test-verified SARS-CoV-2 infection data with time of diagnosis. The present study protocol was approved by the MGB Institutional Review Board (No. 2018P002276).

### Denmark

For the Danish cohort, we combined genotype data from the Copenhagen Hospital Biobank and the Danish Blood Donor Study with

information on SARS-CoV-2 infection from the EFTER-COVID study<sup>49</sup>. In short, the EFTER-COVID study invited individuals older than 15 years of age with a reverse transcription PCR test for SARS-CoV-2 infection between 1 September 2020 and 21 February 2023 to fill in a baseline and several follow-up questionnaires. Cases for SARS-CoV-2 infection with Omicron variants had their first positive test either after 28 December 2021, when more than 90% of new infections were Omicron, or earlier in December 2021, with Omicron infection confirmed by a variant-specific PCR test. Controls were individuals with a negative PCR test related to the EFTER-COVID study and no positive test result for any test in the database. For the comparison with earlier infections, controls were either defined as having a positive test before Omicron infections were observed in Denmark (21 November 2021) or infection with a non-Omicron variant confirmed by variant-specific PCR test in December 2021; individuals with a later re-infection with an Omicron variant were excluded. Basic descriptive statistics on age and sex of cases and controls from all cohorts are given in Supplementary Table 13. Genetic data for the Copenhagen Hospital Biobank and the Danish Blood Donor Study were available from genotyping with Illumina Global Screening Arrays and subsequent imputation were as previously described<sup>50,51</sup>. Data cleaning steps included filtering out individuals who were of non-European genetic ancestries (by removing outliers in a principal component analysis (PCA), deviating more than five standard deviations from one of the first five principal components), related (relatedness coefficient greater than 0.0883), having discordant sex information (chromosome aneuploidies or difference between reported sex and genetically inferred sex), were outliers for heterozygosity or having more than 3% missing genotypes. Case-control GWAS analyses were performed with REGENIE (v.2.2.4)<sup>52</sup> under an additive model, adjusting for sex and the first five principal components. The analyses included 22,041 cases with an Omicron infection, 24,801 controls with no known infection and 18,610 controls with an infection with earlier variants.

### EstBB

The EstBB is a population-based biobank with 212,955 participants in the current data freeze (2024v1). All biobank participants signed a broad informed consent form, and information on ICD-10 codes is obtained by regular linking with the national Health Insurance Fund and other relevant databases, with the majority of the electronic health records having been collected since 2004 (ref. 53). COVID-19 data were acquired from electronic health records (ICD-10 U07\* category), with diagnoses between 1 March 2020 through 30 November 2021 being considered as cases with non-Omicron variants, while cases from 1 January 2022 through 31 December 2022 were considered to be Omicron cases. Participants with diagnoses from both periods were excluded. Controls without any U07\* category diagnoses were considered healthy.

All EstBB participants were genotyped at the Core Genotyping Lab of the Institute of Genomics, University of Tartu, using Illumina Global Screening Array v3.0\_EST. Samples were genotyped and PLINK format files were created using Illumina GenomeStudio (v.2.0.4). Individuals were excluded from the analysis if their call rate was <95%, if they were outliers of the absolute value of heterozygosity (>3 s.d. from the mean) or if sex defined based on heterozygosity of the X chromosome did not match sex in phenotype data<sup>54</sup>. Before imputation, variants were filtered by call rate of <95%, Hardy-Weinberg equilibrium *P* value of  $<1 \times 10^{-4}$  (autosomal variants only) and minor allele frequency of <1%. Genotyped variant positions were in build 37 and were lifted over to build 38 using Picard (v.2.26.2). Phasing was performed using Beagle (v.5.4) software<sup>55</sup>. Imputation was performed with Beagle (v.5.4) software (beagle.22Jul22.46e.jar) and default settings. The dataset was split into batches of 5,000. A population-specific reference panel consisting of 2,695 whole-genome sequencing samples was used for imputation, and standard Beagle hg38 recombination maps were used. Based

on PCA, samples that were not of European ancestry were removed. Duplicate and monozygous twin detection was performed with KING (v.2.2.7)<sup>56</sup>, and one sample was removed from the pair of duplicates.

Association analysis in EstBB was carried out for all variants with an INFO score of  $>0.4$  using the additive model as implemented in REGENIE (v.3.0.3), with standard binary trait settings<sup>52</sup>. Logistic regression was carried out with adjustment for current age, age<sup>2</sup>, sex and ten principal components as covariates, analyzing only variants with a minimum minor allele count of two. The analyses included 61,181 cases with an Omicron infection, 93,852 controls with no known infection and 28,031 controls with an infection with earlier variants.

## FinnGen

Finnish ancestry samples from the Finnish public–private research project FinnGen were used<sup>57</sup>. FinnGen (release 12) comprises genome information with digital healthcare data on ~10% of the Finnish population (<https://www.finngen.fi/en>). Individuals in FinnGen (release 12) with the International Classification of Diseases, Tenth Revision (ICD-10) diagnosis code U07\* for SARS-CoV-2 infection (U07.1 or U07.2, virus identified or not identified, respectively) were defined as SARS-CoV-2-infected. For the GWAS of Omicron, individuals were grouped by the diagnosis date of their first SARS-CoV-2 infection. As Omicron variants became the main lineage in December 2021 in Finland, we defined individuals with their first SARS-CoV-2 diagnosis date starting from 1 January 2022 as Omicron cases ( $n = 61,393$ ). Individuals with no SARS-CoV-2 diagnosis were used as controls ( $n = 399,149$ ). For the comparison with earlier SARS-CoV-2 variants, individuals with diagnosis dates before or in November 2021 and no later re-infection with an Omicron variant were defined as controls ( $n = 35,594$ ). Diagnosis dates in FinnGen data are pseudonymised by  $\pm 2$  weeks; thus, individuals with their first SARS-CoV-2 diagnosis during the Delta–Omicron transition period, December 2021, were excluded from the earlier SARS-CoV-2 controls.

FinnGen samples were genotyped with ThermoFisher, Illumina and Affymetrix arrays. Imputation was performed using the Finnish population-specific imputation panel SISu v4 (v.4.2). FinnGen data (180,000 SNPs) were compared to 1000 Genomes Project data, with a Bayesian algorithm detecting PCA outliers. A total of 35,371 samples were detected as either non-Finnish ancestry or as twins or duplicates with relations to other samples, and thus excluded. Of the 500,737 non-duplicate population inlier samples from PCA, 355 samples were excluded from analysis because of missing minimum phenotype data, and 34 samples were removed because of failing sex check, with F thresholds of 0.4 and 0.7. A total of 500,348 samples (282,064 (56.4%) females and 218,284 (43.6%) males) were accepted for phenotyping for the GWAS analyses.

Case versus control GWAS analyses were performed using REGENIE (v.2.2.4)<sup>52</sup>. Logistic regression was adjusted for age (at death or end of registry follow-up), sex, the first ten principal components and genotyping batches. The Firth approximation test was applied for variants with an initial  $P$  value of  $<0.01$ , and standard error was computed based on the effect size and likelihood ratio test  $P$  value (REGENIE options –firth–approx –pThresh 0.01 –firth-se). The analyses included 61,393 cases with an Omicron infection, 399,149 controls with no known infection and 35,594 controls with an infection with earlier variants.

## MGB Biobank

Cases for SARS-CoV-2 infection with Omicron variants were ascertained from the MGB Biobank (data access 23 April 2024). Individuals with a SARS-CoV-2 infection were curated by the biobank and represent those who presented to the hospital system with a positive infection control flag, presumed infection control flag and/or a SARS-CoV-2 RNA positive test result. Cases of Omicron infections were defined as individuals presenting with a SARS-CoV-2 infection after 1 January 2022. The control definition included individuals in the MGB Biobank

without any report of infection. For the comparison of infections with earlier variants, controls were defined as individuals with a SARS-CoV-2 infection before 1 December 2021 and no later re-infection with an Omicron variant.

The MGB Biobank genotyped 53,297 participants on the Illumina Global Screening Array and 11,864 on Illumina Multi-Ethnic Global Array. The global screening arrays captured approximately 652,000 SNPs and short insertions and deletions, while the multi-ethnic global arrays captured approximately 1.38 million SNPs and short insertions and deletions. These genotypes were filtered for high missingness ( $>2\%$ ) and variants out of Hardy–Weinberg equilibrium ( $P < 1 \times 10^{-12}$ ), as well as variants with an allele frequency discordant ( $P < 1 \times 10^{-150}$ ) from a synthesized allele frequency calculated from GnomAD subpopulation frequencies and a genome-wide GnomAD model fit of the entire cohort. This resulted in approximately 620,000 variants for the global screening array and 1.15 million for the multi-ethnic global array. The two sets of genotypes were then separately phased and imputed on the TOPMed imputation server (Minimac4 algorithm) using the TOPMed r2 reference panel. The resultant imputation sets were both filtered at an  $R^2 > 0.4$  and a minor allele frequency of  $>0.001$ , and then the two sets were merged or intersected, resulting in approximately 19.5 million GRCh38 autosomal variants. The sample set for analysis here was then restricted to just those classified as European according to a random forest classifier trained with the Human Genome Diversity Project as the reference panel, with the minimum probability for assignment to an ancestral group of 0.5, in 19 out of 20 iterations of the model<sup>48</sup>. To correct for population stratification, principal components were computed in genetically European participants. Association analysis was performed with variants using REGENIE (v.3.2.8) with adjustment for age, age<sup>2</sup>, sex, chip, tranche and PC 1–10. The analyses included 7,220 cases with an Omicron infection, 38,843 controls with no known infection and 4,977 controls with an infection with earlier variants.

## Meta-analysis

Initial REGENIE results were filtered based on a minor allele frequency of  $>0.1\%$  and an INFO score of  $>0.8$  and analyzed in METAL (v.2011.03.25)<sup>58</sup> by the inverse-variance method with genomic control applied to the input files. Heterogeneity of the effects across cohorts was tested with the  $\chi^2$  statistic and Cochran's  $Q$ -test for heterogeneity. The results from the meta-analysis were filtered for SNPs present in all three major cohorts, resulting in a total of 8,669,333 SNPs, of which 436,360 did not have results for the MGB cohort (including all 224,900 SNPs from chromosome X).

## LD calculations

When not otherwise stated, LD between SNPs was calculated in LDpair (<https://ldlink.nih.gov/?tab=ldpair>) based on the five European ancestry groups from Utah, Italy, Finland, Great Britain and Spain. In cases for which one of the SNPs was not available in the 1000 Genomes Project reference panel, LD was calculated based on the Danish study cohort.

## Open Targets Genetics analysis

The V2G analysis pipeline in Open Target Genetics<sup>18</sup> provides a single aggregated score for each variant–gene prediction based on four different data types: molecular phenotype quantitative trait loci datasets (expression and protein QTLs), chromatin interaction and conformation datasets, in silico functional predictions (using the Variant Effect Predictor score<sup>59</sup>) and distance from the canonical transcript start site. V2G scores range from zero to one, with higher scores indicating stronger variant–gene links.

## FUMA and MAGMA analyses

FUMA is an integrative web-based platform using information from multiple biological resources to provide functional annotation of GWAS results, positional, expression QTL and chromatin interaction

mappings, gene prioritization and gene-based, pathway and tissue enrichment results<sup>19</sup>. MAGMA is a method developed for gene and gene-set analyses to provide deeper insight into functional and biological mechanisms underlying complex traits<sup>21</sup>. We ran FUMA and the implemented version of MAGMA in one FUMA job (link provided in Data availability).

### MiXeR analysis

To further evaluate the observed genetic correlations between omicron infection and schizophrenia and asthma, we applied univariate and bivariate Gaussian mixture modeling as implemented in MiXeR<sup>26</sup> (v.1.3) to summary statistics for each trait. In its univariate form, MiXeR analyzes GWAS summary statistics by modeling SNP effects as a mixture: combining a point mass at zero (representing non-causal variants) with a continuous distribution for non-zero, causal effects. This enables estimates of polygenicity (the number of causal variants) and discoverability (the variance of their effect sizes). Its bivariate extension simultaneously examines two traits, decomposing their genetic signals into shared and trait-specific components. This joint analysis not only estimates the overall genetic correlation between traits but also quantifies how many causal variants contribute to both traits versus those that are unique.

### STRING functional protein association network analysis

The STRING database compiles and integrates protein–protein associations from various sources to create comprehensive global interaction networks. STRING assigns confidence scores to all protein–protein associations, estimating the likelihood of their accuracy based on available evidence<sup>60</sup>. These precomputed scores range from zero to one and are provided separately for physical and functional associations. To determine these scores, evidence is categorized into seven channels, including co-expression, experimental data, curated databases and text mining. STRING calculates confidence scores for each evidence channel by first quantifying interaction evidence with channel-specific metrics and then converting these into likelihoods using calibration curves based on KEGG pathway data<sup>61</sup>. These scores are then transferred to related protein pairs in other organisms and, finally, a combined confidence score is generated by probabilistically integrating the individual channel scores, assuming their independence. Users can rely on this combined score for network exploration or customize their analyses by enabling or disabling specific channels. STRING also provides a protein–protein interaction enrichment *P* value to investigate whether the proteins in the network exhibit more interactions among themselves than would be expected by chance for a randomly selected, equally sized set of proteins with the same degree (that is, number of connections per protein) distribution from the genome. An independent benchmark has shown that STRING is among the top-performing molecular networks in human disease research<sup>62</sup>.

For our analysis, we obtained functional protein association networks from STRING database v.12 (ref. 61), which we visualized in Cytoscape v.3.10 (ref. 63) using stringApp v.2.1.1 (ref. 64). Initially, we selected one gene per locus (based on candidacy from physical proximity to the lead SNP or additional evidence from FUMA and Open Targets Genetics results) and used the default confidence score threshold of 0.4, indicating medium interaction confidence.

One functionality of STRING is expanding a given network with a user-defined number of interactors at a specific degree of selectivity<sup>64</sup>. We expanded the initial network with 15 interactors, setting the selectivity parameter to the maximum value of 1, allowing us to identify proteins that primarily interact with the current network and are not hubs of the entire STRING network. The genes for some of the 15 retrieved interactors were located at the same locus, or at a locus already represented in the initial network. In these cases, we selected only the entry with the most interactions in the network and removed the other proteins at this locus from the network for our analysis.

### Reporting summary

Further information on research design is available in the Nature Portfolio Reporting Summary linked to this article.

### Data availability

GWAS meta-analysis summary statistics are publicly available for interactive plotting, viewing and downloading through LocusZoom<sup>65</sup> (<https://my.locuszoom.org/gwas/962995>) and are also deposited at the Danish National Biobank (<https://www.danishnationalbiobank.com/gwas/glycosylation-and-omicron-variants>). Complete FUMA results (including the MAGMA analysis) are available online (<https://fuma.ctglab.nl/browse/475677>). The STRING network for 13 genes linked to the GWAS lead SNPs can be found at <https://version-12-0.string-db.org/cgi/network?networkId=bnOf0kS7q9qc>; the STRING network expanded with 15 additional interactors can be found at <https://version-12-0.string-db.org/cgi/network?networkId=bTU3KlbwyQXZ>. Source data are provided with this paper.

### Code availability

Code for the analysis is available at Zenodo (<https://doi.org/10.5281/zenodo.17348245>)<sup>66</sup>.

### References

48. Dashti, H. S. et al. Interaction of obesity polygenic score with lifestyle risk factors in an electronic health record biobank. *BMC Med.* **20**, 5 (2022).
49. Sørensen, A. I. V. et al. Cohort profile: EFTER-COVID—a Danish nationwide cohort for assessing the long-term health effects of the COVID-19 pandemic. *BMJ Open* **14**, e087799 (2024).
50. Sørensen, E. et al. Data Resource Profile: The Copenhagen Hospital Biobank (CHB). *Int. J. Epidemiol.* **50**, 719–720e (2021).
51. Hansen, T. F. et al. DBDS Genomic Cohort, a prospective and comprehensive resource for integrative and temporal analysis of genetic, environmental and lifestyle factors affecting health of blood donors. *BMJ Open* **9**, e028401 (2019).
52. Mbatchou, J. et al. Computationally efficient whole-genome regression for quantitative and binary traits. *Nat. Genet.* **53**, 1097–1103 (2021).
53. Leitsalu, L. et al. Cohort Profile: Estonian Biobank of the Estonian Genome Center, University of Tartu. *Int. J. Epidemiol.* **44**, 1137–1147 (2015).
54. Mitt, M. et al. Improved imputation accuracy of rare and low-frequency variants using population-specific high-coverage WGS-based imputation reference panel. *Eur. J. Hum. Genet.* **25**, 869–876 (2017).
55. Browning, B. L., Tian, X., Zhou, Y. & Browning, S. R. Fast two-stage phasing of large-scale sequence data. *Am. J. Hum. Genet.* **108**, 1880–1890 (2021).
56. Manichaikul, A. et al. Robust relationship inference in genome-wide association studies. *Bioinformatics* **26**, 2867–2873 (2010).
57. Kurki, M. I. et al. FinnGen provides genetic insights from a well-phenotyped isolated population. *Nature* **613**, 508–518 (2023).
58. Willer, C. J., Li, Y. & Abecasis, G. R. METAL: fast and efficient meta-analysis of genome-wide association scans. *Bioinformatics* **26**, 2190–2191 (2010).
59. McLaren, W. et al. The Ensembl Variant Effect Predictor. *Genome Biol.* **17**, 122 (2016).
60. von Mering, C. et al. STRING: known and predicted protein–protein associations, integrated and transferred across organisms. *Nucleic Acids Res.* **33**, D433–D437 (2005).
61. Szklarczyk, D. et al. The STRING database in 2023: protein–protein association networks and functional enrichment analyses for any sequenced genome of interest. *Nucleic Acids Res.* **51**, D638–D646 (2023).

62. Huang, J. K. et al. Systematic evaluation of molecular networks for discovery of disease genes. *Cell Syst.* **6**, 484–495.e5 (2018).
63. Shannon, P. et al. Cytoscape: a software environment for integrated models of biomolecular interaction networks. *Genome Res.* **13**, 2498–2504 (2003).
64. Doncheva, N. T. et al. Cytoscape stringApp 2.0: analysis and visualization of heterogeneous biological networks. *J. Proteome Res.* **22**, 637–646 (2023).
65. Boughton, A. P. et al. LocusZoom.js: interactive and embeddable visualization of genetic association study results. *Bioinformatics* **37**, 3017–3018 (2021).
66. Geller, F. Custom software scripts for Geller et al.: ‘Central role of glycosylation processes in human genetic susceptibility to SARS-CoV-2 infections with Omicron variants’. Zenodo <https://zenodo.org/records/17348245> (2025).

## Acknowledgements

We thank all participants and staff related to the Copenhagen Hospital Biobank, Danish Blood Donor Study, EFTER-COVID, FinnGen, EstBB and MGB Biobank for their contribution to this research. This work was supported in full or in part by the National Institutes of Health (NIH) R01AI170850 (J.V.); Novo Nordisk Foundation NNF22OC0077221 and NNF23OC0087269 (S. Bliddal); NordForsk project nos. 105668 and 138929 (L.A.N.C.); NIH R35GM146839 (J.M.L.) and NIH R01HG012810 (J.M.L.); the Academy of Finland no. 353812 (H.M.O.), NIH R01AI170850 (H.M.O.), EU Horizon Europe research and innovation programme 101057553 (H.M.O.) and the Swiss State Secretariat for Education, Research and Innovation, contract number 22.00094 (H.M.O.); and Novo Nordisk Foundation NNF17OC0027594 (B.F.). This work was also supported by research grants from Sygeforsikringen “danmark” 2020-0178 and the EU Horizon REACT study 101057129. The Copenhagen Hospital Biobank was funded by grants from Novo Nordisk Foundation NNF23OC0082015 and Rigshospitalet Research Council (Framework grant) and by Novo Nordisk Foundation CHALLENGE grant NNF17OC0027594. The Danish Blood Donor Study was funded by the Danish Council for Independent Research—Medical Sciences and the Danish Administrative Regions (Bio- and Genome Bank Denmark). The Danish Departments of Clinical Microbiology and Statens Serum Institut carried out laboratory analyses, registration and release of the national SARS-CoV-2 surveillance data for the present study. The work of the Estonian Genome Center, University of Tartu, was funded by the European Union through the Horizon 2020 research and innovation program under grant nos. 894987, 101137201 and 101137154 and Estonian Research Council Grant PRG1291. The Estonian Genome Center analyses were partially carried out in the High Performance Computing Center, University of Tartu. We acknowledge the participants and investigators of the FinnGen study. The FinnGen project is funded by two grants from Business Finland (HUS 4685/31/2016 and UH 4386/31/2016) and the following industry partners: AbbVie, AstraZeneca UK, Biogen MA, Bristol Myers Squibb (and Celgene Corporation & Celgene International II Sàrl), Genentech, Merck Sharp & Dohme, Pfizer, GlaxoSmithKline Intellectual Property Development, Sanofi US Services, Maze Therapeutics, Janssen Biotech, Novartis and Boehringer Ingelheim International. The following biobanks are acknowledged for delivering biobank samples to FinnGen: Auria Biobank ([www.auria.fi/biopankki](http://www.auria.fi/biopankki)), THL Biobank ([www.thl.fi/biobank](http://www.thl.fi/biobank)),

Helsinki Biobank ([www.helsinginbiopankki.fi](http://www.helsinginbiopankki.fi)), Biobank Borealis of Northern Finland (<https://www.ppshp.fi/Tutkimus-ja-opetus/Biopankki/Pages/Biobank-Borealis-briefly-in-English.aspx>), Finnish Clinical Biobank Tampere ([www.tays.fi/en-US/Research\\_and\\_development/Finnish\\_Clinical\\_Biobank\\_Tampere](http://www.tays.fi/en-US/Research_and_development/Finnish_Clinical_Biobank_Tampere)), Biobank of Eastern Finland ([www.ita-suomenbiopankki.fi/en](http://www.ita-suomenbiopankki.fi/en)), Central Finland Biobank ([www.ksshp.fi/fi-FI/Potilaalle/Biopankki](http://www.ksshp.fi/fi-FI/Potilaalle/Biopankki)), Finnish Red Cross Blood Service Biobank ([www.veripalvelu.fi/verenluovutus/biopankkitoiminta](http://www.veripalvelu.fi/verenluovutus/biopankkitoiminta)), Terveystalo Biobank ([www.terveystalo.com/fi/Yritystietoa/Terveystalo-Biopankki/Biopankki](http://www.terveystalo.com/fi/Yritystietoa/Terveystalo-Biopankki/Biopankki)) and Arctic Biobank (<https://www.oulu.fi/en/university/faculties-and-units/faculty-medicine/northern-finland-birth-cohorts-and-arctic-biobank>). All Finnish Biobanks are members of BBMRI.fi infrastructure (<https://www.bbMRI-ERIC.eu/national-nodes/finland>). Finnish Biobank Cooperative—FINBB (<https://finbb.fi>) is the coordinator of BBMRI-ERIC operations in Finland. The Finnish biobank data can be accessed through the Fingenious services (<https://site.fingenious.fi/en>) managed by FINBB. We thank the MGB Biobank for providing samples, genomic data and health information data for genetic analyses.

## Author contributions

F.G. conceptualized the study, coordinated the analyses and wrote the first manuscript draft. F.G., X.W., V.L., E.A., H.M.O. and B.F. designed the analyses and interpreted the results. F.G., X.W., V.L., E.A., J.T.V., K.N., A.B., N.W.A., L.Q. and J.M.L. analyzed the data. M.R. and R.L. interpreted results in the context of viral immunology. B.A., K.B., S. Bliddal, L.B., S. Brunak, N.B., J.B.-G., L.A.N.C., M.D., K.M.D., C.E., U.F.-R., K.G., K.A.K., C.M., C.H.N., H.S.N., S.D.N., J.N., C.B.S., N.T., H.U., L.S., P.B., A.H., E.S., O.B.P. and S.R.O. provided data from the Danish study groups. H.M.O., S.R.O. and B.F. jointly supervised the study. All authors contributed to the final manuscript.

## Competing interests

S. Brunak has ownerships in Intomics, Hoba Therapeutics, Novo Nordisk, Lundbeck, ALK abello, Eli Lilly and Co. and managing board memberships in Proscion and Intomics. C.E. has received unrestricted research grants from Novo Nordisk, administered by Aarhus University, and Abbott Diagnostics, administered by Aarhus University Hospital. C.E. received no personal fees. K.G. received a Janssen Pharma research grant and is on the advisory board of Otsuka Pharma. L.B. currently works for MSD Denmark. All other authors report no competing interests.

## Additional information

**Supplementary information** The online version contains supplementary material available at <https://doi.org/10.1038/s41588-025-02484-9>.

**Correspondence and requests for materials** should be addressed to Frank Geller.

**Peer review information** *Nature Genetics* thanks Manuel Ferreira, Janie Shelton and the other, anonymous, reviewer(s) for their contribution to the peer review of this work. Peer reviewer reports are available.

**Reprints and permissions information** is available at [www.nature.com/reprints](http://www.nature.com/reprints).

## Reporting Summary

Nature Portfolio wishes to improve the reproducibility of the work that we publish. This form provides structure for consistency and transparency in reporting. For further information on Nature Portfolio policies, see our [Editorial Policies](#) and the [Editorial Policy Checklist](#).

### Statistics

For all statistical analyses, confirm that the following items are present in the figure legend, table legend, main text, or Methods section.

n/a Confirmed

- The exact sample size ( $n$ ) for each experimental group/condition, given as a discrete number and unit of measurement
- A statement on whether measurements were taken from distinct samples or whether the same sample was measured repeatedly
- The statistical test(s) used AND whether they are one- or two-sided
  - Only common tests should be described solely by name; describe more complex techniques in the Methods section.*
- A description of all covariates tested
- A description of any assumptions or corrections, such as tests of normality and adjustment for multiple comparisons
- A full description of the statistical parameters including central tendency (e.g. means) or other basic estimates (e.g. regression coefficient) AND variation (e.g. standard deviation) or associated estimates of uncertainty (e.g. confidence intervals)
- For null hypothesis testing, the test statistic (e.g.  $F$ ,  $t$ ,  $r$ ) with confidence intervals, effect sizes, degrees of freedom and  $P$  value noted
  - Give  $P$  values as exact values whenever suitable.*
- For Bayesian analysis, information on the choice of priors and Markov chain Monte Carlo settings
- For hierarchical and complex designs, identification of the appropriate level for tests and full reporting of outcomes
- Estimates of effect sizes (e.g. Cohen's  $d$ , Pearson's  $r$ ), indicating how they were calculated

*Our web collection on [statistics for biologists](#) contains articles on many of the points above.*

### Software and code

Policy information about [availability of computer code](#)

Data collection	No software was used for data collection.
Data analysis	<p>GWAS analyses were performed using REGENIE (versions 2.2.4, 3.0.3, 3.2.8). LD between SNPs was calculated in LDpair (<a href="https://ldlink.nih.gov/?tab=ldpair">https://ldlink.nih.gov/?tab=ldpair</a>). Meta-analyses were performed in METAL (version 2011.03.25). Open Targets Genetics analysis was performed by putting the 13 lead SNPs forward to the web tool (<a href="https://genetics.opentargets.org/">https://genetics.opentargets.org/</a>), accession date January 20, 2025). FUMA (v1.5.2) and MAGMA (v1.08) analyses were performed for the GWAS of Omicron infection and can be accessed through the FUMA site (<a href="https://fuma.ctglab.nl/browse/475677">https://fuma.ctglab.nl/browse/475677</a>). MiXeR (v1.3) analyses were performed for GWAS summary statistics of Omicron infection, schizophrenia and asthma. WGWA analyses were performed using REGENIE (versions 2.2.4, 3.0.3, 3.2.8). LD between SNPs was calculated in LDpair (<a href="https://ldlink.nih.gov/?tab=ldpair">https://ldlink.nih.gov/?tab=ldpair</a>). Meta-analyses were performed in METAL (version 2011.03.25). Open Targets Genetics analysis was performed by putting the 13 lead SNPs forward to the web tool (<a href="https://genetics.opentargets.org/">https://genetics.opentargets.org/</a>), accession date January 20, 2025). FUMA (v1.5.2) and MAGMA (v1.08) analyses were performed for the GWAS of Omicron infection and can be accessed through the FUMA site (<a href="https://fuma.ctglab.nl/browse/475677">https://fuma.ctglab.nl/browse/475677</a>). MiXeR (v1.3) analyses were performed for GWAS summary statistics of Omicron infection, schizophrenia and asthma. We obtained functional protein association networks from STRING database v12, which we visualized in Cytoscape v3.10 using stringApp v2.1.1.</p>

e obtained functional protein association networks from STRING database v12, which we visualized in Cytoscape v3.10 using stringApp v2.1.1.

For manuscripts utilizing custom algorithms or software that are central to the research but not yet described in published literature, software must be made available to editors and reviewers. We strongly encourage code deposition in a community repository (e.g. GitHub). See the Nature Portfolio [guidelines for submitting code & software](#) for further information.

## Data

Policy information about [availability of data](#)

All manuscripts must include a [data availability statement](#). This statement should provide the following information, where applicable:

- Accession codes, unique identifiers, or web links for publicly available datasets
- A description of any restrictions on data availability
- For clinical datasets or third party data, please ensure that the statement adheres to our [policy](#)

GWAS meta-analysis summary statistics are publicly available for interactive plotting, viewing and downloading via LocusZoom65 (<https://my.locuszoom.org/gwas/962995>), and are also deposited at the Danish National Biobank (<https://www.danishnationalbiobank.com/gwas/glycosylation-and-omicron-variants>). Complete FUMA results (including the MAGMA analysis) are available online (<https://fuma.ctglab.nl/browse/475677>).

STRING network for 13 genes linked to the GWAS lead SNPs:

<https://version-12.0.string-db.org/cgi/network?networkId=bnOf0kS7q9qc>.

STRING network expanded with 15 additional interactors:

<https://version-12.0.string-db.org/cgi/network?networkId=bTU3KlbwyQXZ>.

## Research involving human participants, their data, or biological material

Policy information about studies with [human participants or human data](#). See also policy information about [sex, gender \(identity/presentation\), and sexual orientation](#) and [race, ethnicity and racism](#).

Reporting on sex and gender

GWAS were performed with biological sex as covariate.

Reporting on race, ethnicity, or other socially relevant groupings

The large majority of individuals in the study cohorts were of European ancestry (based on the genetic data), and we therefore restricted the analyses to European ancestry individuals.

Population characteristics

Denmark

For the Danish cohort we combined genotype data from the Copenhagen Hospital Biobank and the Danish Blood Donor Study with information on SARS-CoV-2 infection from the EFTER-COVID study. The 22,041 individuals with Omicron infections had a mean age of 49.52 (SD 15.89) years. The 24,814 individuals with no known infection had a mean age of 54.73 (SD 16.35) years. The 18,610 individuals with pre-Omicron infections had a mean age of 48.36 (SD 15.45) years.

Estonian Biobank

The Estonian Biobank (EstBB) is a population-based biobank with 212,955 participants in the current data freeze (2024v1). The 61,181 individuals with Omicron infections had a mean age of 49.06 (SD 14.93) years. The 93,852 individuals with no known infection had a mean age of 55.58 (SD 17.77) years. The 28,031 individuals with pre-Omicron infections had a mean age of 48.50 (SD 14.84) years.

FinnGen

FinnGen is a Finnish public-private research project. FinnGen release 12 comprises genome information with digital healthcare data on ~10% of Finnish population (<https://www.finngen.fi/en>). The 61,393 individuals with Omicron infections had a mean age of 52.05 (SD 16.07) years. The 399,149 individuals with no known infection had a mean age of 63.38 (SD 17.61) years. The 35,594 individuals with pre-Omicron infections had a mean age of 48.37 (SD 15.60) years.

Mass General Brigham Biobank

The Mass General Brigham (MGB) Biobank, is a hospital-based cohort study produced by the MGB healthcare network located in Boston, MA. The 7,220 individuals with Omicron infections had a mean age of 62.55 (SD 15.40) years. The 38,843 individuals with no known infection had a mean age of 60.60 (SD 17.14) years. The 4,977 individuals with pre-Omicron infections had a mean age of 57.23 (SD 16.43) years.

Recruitment

The study was built on existing cohorts, there was no recruitment specifically for this study.

Ethics oversight

The Copenhagen Hospital Biobank provides biological left-over samples from routine blood analyses and the patients were not asked for informed consent before inclusion. Instead, patients were informed about the opt-out possibility to have their biological specimens excluded from use in research. Individuals from the exclusion register (Vævsanvendelsesregistret) were excluded from the study. For the Danish Blood Donor Study, informed consent was obtained from all participants. Both studies are part of a COVID-19 protocol approved by the National Ethics Committee (H-21030945) and the Danish Data Protection Agency (P-2020-356).

EFTER-COVID was conducted as a surveillance study as part of Statens Serum Institut's advisory tasks for the Danish Ministry of Health. According to Danish law, these national surveillance activities do not require approval from an ethics committee. Participation in the study was voluntary and the invitation letter contained information about participants' rights under the Danish General Data Protection Regulation (rights to access data, rectification, deletion, restriction of processing and objection). After reading this information, it was considered informed consent when participants read the information and agreed, and then continued to fill in the questionnaires.

The activities of the Estonian Biobank (EstBB) are regulated by the Human Genes Research Act, which was adopted in 2000 specifically for the operations of EstBB. Individual level analysis with EstBB data was carried out under ethical approval 1.1-12/624 from the Estonian Committee on Bioethics and Human Research (Estonian Ministry of Social Affairs), using data according to release application 6-7/GI/5933 from the Estonian Biobank.

Study subjects in FinnGen provided informed consent for biobank research, based on the Finnish Biobank Act. Alternatively, separate research cohorts, collected prior the Finnish Biobank Act came into effect (in September 2013) and start of FinnGen (August 2017), were collected based on study-specific consents and later transferred to the Finnish biobanks after approval by Fimea (Finnish Medicines Agency), the National Supervisory Authority for Welfare and Health. Recruitment protocols followed the biobank protocols approved by Fimea. The Coordinating Ethics Committee of the Hospital District of Helsinki and Uusimaa (HUS) statement number for the FinnGen study is Nr HUS/990/2017. The FinnGen study is approved by the Finnish Institute for Health and Welfare and other authorities.

The Mass General Brigham (MGB) Biobank, formerly known as the Partners Biobank, is a hospital-based cohort study produced by the MGB healthcare network located in Boston, MA. The MGB Biobank contains data from patients in multiple primary care facilities, as well as tertiary care centers located in the greater Boston area. Participants of the study are recruited from inpatient stays, emergency department environments, outpatient visits, and through a secure online portal available to patients. Recruitment and consent are fully translatable to Spanish in order to promote a greater patient diversity. This allows for a systematic enrollment of diverse patient groups which is reflective of the population receiving care through the MGB network. Recruitment for the biobank began in 2009 and is still actively recruiting. The recruitment strategy has been described previously<sup>51</sup>. For the MGB Biobank, all patients provide written consent upon enrollment. Furthermore, the MGB cohort included test verified SARS-CoV-2 infection data with time of diagnosis. The present study protocol was approved by the MGB Institutional Review Board (#2018P002276).

Note that full information on the approval of the study protocol must also be provided in the manuscript.

## Field-specific reporting

Please select the one below that is the best fit for your research. If you are not sure, read the appropriate sections before making your selection.

Life sciences       Behavioural & social sciences       Ecological, evolutionary & environmental sciences

For a reference copy of the document with all sections, see [nature.com/documents/nr-reporting-summary-flat.pdf](https://nature.com/documents/nr-reporting-summary-flat.pdf)

### Life sciences study design

All studies must disclose on these points even when the disclosure is negative.

Sample size	151,835 individuals with SARS-CoV-2 Omicron infection, (98,015 females, 53,820 males) 556,658 individuals with no known SARS-CoV-2 infection, (307,346 females, 249,312 males) 87,212 individuals with SARS-CoV-2 pre-Omicron infection, (55,548 females, 31,664 males)
Data exclusions	The study was restricted to individuals of European ancestry.
Replication	No replication.
Randomization	No randomization.
Blinding	No blinding.

### Behavioural & social sciences study design

All studies must disclose on these points even when the disclosure is negative.

Study description	Briefly describe the study type including whether data are quantitative, qualitative, or mixed-methods (e.g. qualitative cross-sectional, quantitative experimental, mixed-methods case study).
Research sample	State the research sample (e.g. Harvard university undergraduates, villagers in rural India) and provide relevant demographic information (e.g. age, sex) and indicate whether the sample is representative. Provide a rationale for the study sample chosen. For studies involving existing datasets, please describe the dataset and source.
Sampling strategy	Describe the sampling procedure (e.g. random, snowball, stratified, convenience). Describe the statistical methods that were used to predetermine sample size OR if no sample-size calculation was performed, describe how sample sizes were chosen and provide a rationale for why these sample sizes are sufficient. For qualitative data, please indicate whether data saturation was considered, and what criteria were used to decide that no further sampling was needed.
Data collection	Provide details about the data collection procedure, including the instruments or devices used to record the data (e.g. pen and paper, computer, eye tracker, video or audio equipment) whether anyone was present besides the participant(s) and the researcher, and whether the researcher was blind to experimental condition and/or the study hypothesis during data collection.
Timing	Indicate the start and stop dates of data collection. If there is a gap between collection periods, state the dates for each sample cohort.
Data exclusions	If no data were excluded from the analyses, state so OR if data were excluded, provide the exact number of exclusions and the rationale behind them, indicating whether exclusion criteria were pre-established.

**Non-participation** State how many participants dropped out/declined participation and the reason(s) given OR provide response rate OR state that no participants dropped out/declined participation.

**Randomization** If participants were not allocated into experimental groups, state so OR describe how participants were allocated to groups, and if allocation was not random, describe how covariates were controlled.

## Ecological, evolutionary & environmental sciences study design

All studies must disclose on these points even when the disclosure is negative.

**Study description** Briefly describe the study. For quantitative data include treatment factors and interactions, design structure (e.g. factorial, nested, hierarchical), nature and number of experimental units and replicates.

**Research sample** Describe the research sample (e.g. a group of tagged *Passer domesticus*, all *Stenocereus thurberi* within Organ Pipe Cactus National Monument), and provide a rationale for the sample choice. When relevant, describe the organism taxa, source, sex, age range and any manipulations. State what population the sample is meant to represent when applicable. For studies involving existing datasets, describe the data and its source.

**Sampling strategy** Note the sampling procedure. Describe the statistical methods that were used to predetermine sample size OR if no sample-size calculation was performed, describe how sample sizes were chosen and provide a rationale for why these sample sizes are sufficient.

**Data collection** Describe the data collection procedure, including who recorded the data and how.

**Timing and spatial scale** Indicate the start and stop dates of data collection, noting the frequency and periodicity of sampling and providing a rationale for these choices. If there is a gap between collection periods, state the dates for each sample cohort. Specify the spatial scale from which the data are taken

**Data exclusions** If no data were excluded from the analyses, state so OR if data were excluded, describe the exclusions and the rationale behind them, indicating whether exclusion criteria were pre-established.

**Reproducibility** Describe the measures taken to verify the reproducibility of experimental findings. For each experiment, note whether any attempts to repeat the experiment failed OR state that all attempts to repeat the experiment were successful.

**Randomization** Describe how samples/organisms/participants were allocated into groups. If allocation was not random, describe how covariates were controlled. If this is not relevant to your study, explain why.

**Blinding** Describe the extent of blinding used during data acquisition and analysis. If blinding was not possible, describe why OR explain why blinding was not relevant to your study.

Did the study involve field work?  Yes  No

## Field work, collection and transport

**Field conditions** Describe the study conditions for field work, providing relevant parameters (e.g. temperature, rainfall).

**Location** State the location of the sampling or experiment, providing relevant parameters (e.g. latitude and longitude, elevation, water depth).

**Access & import/export** Describe the efforts you have made to access habitats and to collect and import/export your samples in a responsible manner and in compliance with local, national and international laws, noting any permits that were obtained (give the name of the issuing authority, the date of issue, and any identifying information).

**Disturbance** Describe any disturbance caused by the study and how it was minimized.

## Reporting for specific materials, systems and methods

We require information from authors about some types of materials, experimental systems and methods used in many studies. Here, indicate whether each material, system or method listed is relevant to your study. If you are not sure if a list item applies to your research, read the appropriate section before selecting a response.

## Materials & experimental systems

n/a	Involved in the study
<input checked="" type="checkbox"/>	Antibodies
<input checked="" type="checkbox"/>	Eukaryotic cell lines
<input checked="" type="checkbox"/>	Palaeontology and archaeology
<input checked="" type="checkbox"/>	Animals and other organisms
<input checked="" type="checkbox"/>	Clinical data
<input checked="" type="checkbox"/>	Dual use research of concern
<input checked="" type="checkbox"/>	Plants

## Methods

n/a	Involved in the study
<input checked="" type="checkbox"/>	ChIP-seq
<input checked="" type="checkbox"/>	Flow cytometry
<input checked="" type="checkbox"/>	MRI-based neuroimaging

## Antibodies

### Antibodies used

Describe all antibodies used in the study; as applicable, provide supplier name, catalog number, clone name, and lot number.

### Validation

Describe the validation of each primary antibody for the species and application, noting any validation statements on the manufacturer's website, relevant citations, antibody profiles in online databases, or data provided in the manuscript.

## Eukaryotic cell lines

### Policy information about [cell lines and Sex and Gender in Research](#)

#### Cell line source(s)

State the source of each cell line used and the sex of all primary cell lines and cells derived from human participants or vertebrate models.

#### Authentication

Describe the authentication procedures for each cell line used OR declare that none of the cell lines used were authenticated.

#### Mycoplasma contamination

Confirm that all cell lines tested negative for mycoplasma contamination OR describe the results of the testing for mycoplasma contamination OR declare that the cell lines were not tested for mycoplasma contamination.

#### Commonly misidentified lines (See [ICLAC register](#))

Name any commonly misidentified cell lines used in the study and provide a rationale for their use.

## Palaeontology and Archaeology

### Specimen provenance

Provide provenance information for specimens and describe permits that were obtained for the work (including the name of the issuing authority, the date of issue, and any identifying information). Permits should encompass collection and, where applicable, export.

### Specimen deposition

Indicate where the specimens have been deposited to permit free access by other researchers.

### Dating methods

If new dates are provided, describe how they were obtained (e.g. collection, storage, sample pretreatment and measurement), where they were obtained (i.e. lab name), the calibration program and the protocol for quality assurance OR state that no new dates are provided.

Tick this box to confirm that the raw and calibrated dates are available in the paper or in Supplementary Information.

### Ethics oversight

Identify the organization(s) that approved or provided guidance on the study protocol, OR state that no ethical approval or guidance was required and explain why not.

Note that full information on the approval of the study protocol must also be provided in the manuscript.

## Animals and other research organisms

### Policy information about [studies involving animals; ARRIVE guidelines](#) recommended for reporting animal research, and [Sex and Gender in Research](#)

#### Laboratory animals

For laboratory animals, report species, strain and age OR state that the study did not involve laboratory animals.

#### Wild animals

Provide details on animals observed in or captured in the field; report species and age where possible. Describe how animals were caught and transported and what happened to captive animals after the study (if killed, explain why and describe method; if released, say where and when) OR state that the study did not involve wild animals.

#### Reporting on sex

Indicate if findings apply to only one sex; describe whether sex was considered in study design, methods used for assigning sex. Provide data disaggregated for sex where this information has been collected in the source data as appropriate; provide overall

numbers in this Reporting Summary. Please state if this information has not been collected. Report sex-based analyses where performed, justify reasons for lack of sex-based analysis.

**Field-collected samples** For laboratory work with field-collected samples, describe all relevant parameters such as housing, maintenance, temperature, photoperiod and end-of-experiment protocol OR state that the study did not involve samples collected from the field.

**Ethics oversight** Identify the organization(s) that approved or provided guidance on the study protocol, OR state that no ethical approval or guidance was required and explain why not.

Note that full information on the approval of the study protocol must also be provided in the manuscript.

## Clinical data

Policy information about [clinical studies](#)

All manuscripts should comply with the ICMJE [guidelines for publication of clinical research](#) and a completed [CONSORT checklist](#) must be included with all submissions.

**Clinical trial registration** Provide the trial registration number from ClinicalTrials.gov or an equivalent agency.

**Study protocol** Note where the full trial protocol can be accessed OR if not available, explain why.

**Data collection** Describe the settings and locales of data collection, noting the time periods of recruitment and data collection.

**Outcomes** Describe how you pre-defined primary and secondary outcome measures and how you assessed these measures.

## Dual use research of concern

Policy information about [dual use research of concern](#)

### Hazards

Could the accidental, deliberate or reckless misuse of agents or technologies generated in the work, or the application of information presented in the manuscript, pose a threat to:

No	Yes
<input checked="" type="checkbox"/>	<input type="checkbox"/> Public health
<input checked="" type="checkbox"/>	<input type="checkbox"/> National security
<input checked="" type="checkbox"/>	<input type="checkbox"/> Crops and/or livestock
<input checked="" type="checkbox"/>	<input type="checkbox"/> Ecosystems
<input checked="" type="checkbox"/>	<input type="checkbox"/> Any other significant area

### Experiments of concern

Does the work involve any of these experiments of concern:

No	Yes
<input checked="" type="checkbox"/>	<input type="checkbox"/> Demonstrate how to render a vaccine ineffective
<input checked="" type="checkbox"/>	<input type="checkbox"/> Confer resistance to therapeutically useful antibiotics or antiviral agents
<input checked="" type="checkbox"/>	<input type="checkbox"/> Enhance the virulence of a pathogen or render a nonpathogen virulent
<input checked="" type="checkbox"/>	<input type="checkbox"/> Increase transmissibility of a pathogen
<input checked="" type="checkbox"/>	<input type="checkbox"/> Alter the host range of a pathogen
<input checked="" type="checkbox"/>	<input type="checkbox"/> Enable evasion of diagnostic/detection modalities
<input checked="" type="checkbox"/>	<input type="checkbox"/> Enable the weaponization of a biological agent or toxin
<input checked="" type="checkbox"/>	<input type="checkbox"/> Any other potentially harmful combination of experiments and agents

## Plants

Seed stocks	Report on the source of all seed stocks or other plant material used. If applicable, state the seed stock centre and catalogue number. If plant specimens were collected from the field, describe the collection location, date and sampling procedures.
Novel plant genotypes	Describe the methods by which all novel plant genotypes were produced. This includes those generated by transgenic approaches, gene editing, chemical/radiation-based mutagenesis and hybridization. For transgenic lines, describe the transformation method, the number of independent lines analyzed and the generation upon which experiments were performed. For gene-edited lines, describe the editor used, the endogenous sequence targeted for editing, the targeting guide RNA sequence (if applicable) and how the editor was applied.
Authentication	Describe any authentication procedures for each seed stock used or novel genotype generated. Describe any experiments used to assess the effect of a mutation and, where applicable, how potential secondary effects (e.g. second site T-DNA insertions, mosaicism, off-target gene editing) were examined.

## ChIP-seq

### Data deposition

- Confirm that both raw and final processed data have been deposited in a public database such as [GEO](#).
- Confirm that you have deposited or provided access to graph files (e.g. BED files) for the called peaks.

#### Data access links

*May remain private before publication.*

For "Initial submission" or "Revised version" documents, provide reviewer access links. For your "Final submission" document, provide a link to the deposited data.

#### Files in database submission

Provide a list of all files available in the database submission.

#### Genome browser session (e.g. [UCSC](#))

Provide a link to an anonymized genome browser session for "Initial submission" and "Revised version" documents only, to enable peer review. Write "no longer applicable" for "Final submission" documents.

### Methodology

Replicates	Describe the experimental replicates, specifying number, type and replicate agreement.
Sequencing depth	Describe the sequencing depth for each experiment, providing the total number of reads, uniquely mapped reads, length of reads and whether they were paired- or single-end.
Antibodies	Describe the antibodies used for the ChIP-seq experiments; as applicable, provide supplier name, catalog number, clone name, and lot number.
Peak calling parameters	Specify the command line program and parameters used for read mapping and peak calling, including the ChIP, control and index files used.
Data quality	Describe the methods used to ensure data quality in full detail, including how many peaks are at FDR 5% and above 5-fold enrichment.
Software	Describe the software used to collect and analyze the ChIP-seq data. For custom code that has been deposited into a community repository, provide accession details.

## Flow Cytometry

### Plots

Confirm that:

- The axis labels state the marker and fluorochrome used (e.g. CD4-FITC).
- The axis scales are clearly visible. Include numbers along axes only for bottom left plot of group (a 'group' is an analysis of identical markers).
- All plots are contour plots with outliers or pseudocolor plots.
- A numerical value for number of cells or percentage (with statistics) is provided.

### Methodology

Sample preparation	Describe the sample preparation, detailing the biological source of the cells and any tissue processing steps used.
Instrument	Identify the instrument used for data collection, specifying make and model number.
Software	Describe the software used to collect and analyze the flow cytometry data. For custom code that has been deposited into a community repository, provide accession details.

**Cell population abundance** *Describe the abundance of the relevant cell populations within post-sort fractions, providing details on the purity of the samples and how it was determined.*

**Gating strategy** *Describe the gating strategy used for all relevant experiments, specifying the preliminary FSC/SSC gates of the starting cell population, indicating where boundaries between "positive" and "negative" staining cell populations are defined.*

Tick this box to confirm that a figure exemplifying the gating strategy is provided in the Supplementary Information.

## Magnetic resonance imaging

### Experimental design

**Design type** *Indicate task or resting state; event-related or block design.*

**Design specifications** *Specify the number of blocks, trials or experimental units per session and/or subject, and specify the length of each trial or block (if trials are blocked) and interval between trials.*

**Behavioral performance measures** *State number and/or type of variables recorded (e.g. correct button press, response time) and what statistics were used to establish that the subjects were performing the task as expected (e.g. mean, range, and/or standard deviation across subjects).*

### Acquisition

**Imaging type(s)** *Specify: functional, structural, diffusion, perfusion.*

**Field strength** *Specify in Tesla*

**Sequence & imaging parameters** *Specify the pulse sequence type (gradient echo, spin echo, etc.), imaging type (EPI, spiral, etc.), field of view, matrix size, slice thickness, orientation and TE/TR/flip angle.*

**Area of acquisition** *State whether a whole brain scan was used OR define the area of acquisition, describing how the region was determined.*

**Diffusion MRI**  Used  Not used

### Preprocessing

**Preprocessing software** *Provide detail on software version and revision number and on specific parameters (model/functions, brain extraction, segmentation, smoothing kernel size, etc.).*

**Normalization** *If data were normalized/standardized, describe the approach(es): specify linear or non-linear and define image types used for transformation OR indicate that data were not normalized and explain rationale for lack of normalization.*

**Normalization template** *Describe the template used for normalization/transformation, specifying subject space or group standardized space (e.g. original Talairach, MNI305, ICBM152) OR indicate that the data were not normalized.*

**Noise and artifact removal** *Describe your procedure(s) for artifact and structured noise removal, specifying motion parameters, tissue signals and physiological signals (heart rate, respiration).*

**Volume censoring** *Define your software and/or method and criteria for volume censoring, and state the extent of such censoring.*

### Statistical modeling & inference

**Model type and settings** *Specify type (mass univariate, multivariate, RSA, predictive, etc.) and describe essential details of the model at the first and second levels (e.g. fixed, random or mixed effects; drift or auto-correlation).*

**Effect(s) tested** *Define precise effect in terms of the task or stimulus conditions instead of psychological concepts and indicate whether ANOVA or factorial designs were used.*

**Specify type of analysis:**  Whole brain  ROI-based  Both

**Statistic type for inference** *Specify voxel-wise or cluster-wise and report all relevant parameters for cluster-wise methods.*

(See [Eklund et al. 2016](#))

**Correction** *Describe the type of correction and how it is obtained for multiple comparisons (e.g. FWE, FDR, permutation or Monte Carlo).*

## Models & analysis

n/a	Involved in the study
<input checked="" type="checkbox"/>	<input type="checkbox"/> Functional and/or effective connectivity
<input checked="" type="checkbox"/>	<input type="checkbox"/> Graph analysis
<input checked="" type="checkbox"/>	<input type="checkbox"/> Multivariate modeling or predictive analysis

### Functional and/or effective connectivity

*Report the measures of dependence used and the model details (e.g. Pearson correlation, partial correlation, mutual information).*

### Graph analysis

*Report the dependent variable and connectivity measure, specifying weighted graph or binarized graph, subject- or group-level, and the global and/or node summaries used (e.g. clustering coefficient, efficiency, etc.).*

### Multivariate modeling and predictive analysis

*Specify independent variables, features extraction and dimension reduction, model, training and evaluation metrics.*